THE IMPACT OF INTERLEUKIN-6 ON THE METABOLIC RESPONSE TO ENDOTOXIN *in vivo*

By

Andrea Donielle Tweedell

Thesis

Submitted to the Faculty of the

Graduate School of Vanderbilt University

in partial fulfillment of the requirements

for the degree of

MASTER OF SCIENCE

in

Molecular Physiology and Biophysics

August, 2005

Nashville, Tennessee

Approved:

David Wasserman

Owen M^{c}Guinness

Mary Courtney Moore

Masakazu Shiota

MOLECULAR PHYSIOLOGY AND BIOPHYSICS

THE IMPACT OF INTERLEUKIN-6 ON THE METABOLIC RESPONSE TO ENDOTOXIN *in vivo*

ANDREA DONIELLE TWEEDELL

Thesis under the direction of Professor Owen P. M^{c}Guinness

Inflammation and insulin resistance are characteristics of endotoxemia. While the role of interleukin-6 (IL-6) in insulin resistant states has been characterized, little is known of its role in the metabolic response to inflammation. To study the role of IL-6, conscious chronically catheterized mice were used. Five days prior to being studied, catheters were implanted in the carotid artery and jugular vein. After a 5 h fast, *E.coli* (250 μg/mouse) LPS was injected in $IL6^{-/-}$ (KO; n=13), $IL6^{+/-}$ (HET; n=9), and $IL\text{-}6^{+/+}$ (WT; n=10) littermates. The IL-6 response to LPS was simulated in an additional group of KO mice (KO+IL6; n=10). Glucose turnover (R_a) was assessed using 3-[^{3}H]-D-glucose. IL-6 increased similarly in WT and HET (15±0.7 and 14±0.5 ng/ml) 4h after LPS and was undetectable in KO. IL-6 replacement in KO restored circulating IL-6 to levels observed in the WT group (14±0.3 ng/ml). WT was the only group to experience an early rise in tumor necrosis factor-α (TNF-α). Interleukin-1β (IL-1β) was similar in all groups. KO exhibited a more profound hyperglycemia 30 min after LPS injection and no apparent hypoglycemia at 4h (95±5 mg/dl). Glucose levels in KO+IL6, while decreased (93±4 mg/dl) at 4h, remained higher than WT. R_a was not altered. In summary, the absence of

IL-6 protected against LPS induced hypoglycemia. Acute restoration of the IL-6 response to LPS did not potentiate hypoglycemia. Thus, while IL-6 promotes glucose intolerance in insulin resistant states, IL-6 promotes hypoglycemia during inflammation.

To my number one fan, Shawn, you are my soul mate and the love of my life

and

To my beautiful daughter, Darian, I love you so much

ACKNOWLEDGEMENTS

There are so many people who have encouraged me, inspired me, and stood by me as I traveled down this scholastic road, I want to thank you all.

First, I would like to thank Owen M^{c}Guinness for being an outstanding mentor. I am truly grateful for the time and energy he has spent guiding me. He has been instrumental in molding me into the scientist I am today. Second, I would like to thank David Wasserman for always lending an ear and offering valuable scientific advice when I needed it. My thesis committee, Masa Shiota, Genie Moore, and David Wasserman, have contributed amazing feedback on this project and have helped me immensely. I would also like to thank Carlo Malabanan and Deanna "Bing" Bracy for their surgical expertise, patience with my study schedule, and listening to my babble.

The members of my laboratory have been an outstanding support unit and wonderful friends. Thanks so much to Tammy Santomango, Fu-Yu Chueh, Sheng-Song Chen, Kimberly Mulligan, Jane Shearer, Pat Fueger, Julio Ayala, Rich Pencek, Raul Camacho, and Freyja James for always making the lab enjoyable. Thanks especially to Pat and Julio for giving me valuable insight on my project. Jamie Yates, Tasneem Ansari, Jessica Potts, and Anna Wilson of the Mouse Metabolic Phenotyping Center, summer student Yossi Martel, and Eric Allen, Wanda Snead, and Angela Slater of the Hormone Assay Core have all played a vital role in carrying out this work.

Last but definitely not least, none of this would have been possible without the unwavering support and love from my husband Shawn and my amazing family. I cannot

even begin to thank God enough for blessing me with the most wonderful husband and family in the world. Thank you.

TABLE OF CONTENTS

LIST OF FIGURES

CHAPTER I

INTRODUCTION

The pathogenic effects of gram-negative bacteria are primarily brought about by exposure within the mammalian host to the bacterial endotoxic component called lipopolysaccharide (LPS). Exposure to LPS results in a subsequent chain of events that varies widely but can consist of infection, the systemic inflammatory response syndrome (SIRS) plus infection, septic shock, multiple organ dysfunction syndrome (MODS) and eventually death (93). Sepsis, or endotoxemia, has been described as "an infection-induced syndrome defined as the presence of two or more of the following features of systemic inflammation: fever or hypothermia, leukocytosis or leucopenia, tachycardia, and tachypnea or a supranormal minute ventilation" (13). Severe sepsis is defined as sepsis accompanied by acute organ dysfunction (64). Epidemiological analysis yields estimates of roughly 750,000 cases of severe sepsis occur in the United States per year (3). Crude mortality rates resulting from severe sepsis range from 28% to 50% and are considered unacceptably high (3).

There are multiple hurdles involved in the adequate treatment of hospitalized patients with septicemia; the most profound is the difficulty in choosing a proper therapeutic regimen. This arises because of the complicated nature of evaluating investigational agents in patients with severe sepsis (64). There are multiple reasons for this problem, to include:

- the heterogeneity of the syndrome and patient population
- lack of translated success from animal model to human
- patients present with more complicated than simple endotoxin challenge
- the immunopathogenesis is a complex and dynamic process
- coagulation issues
- multiple influences on the outcome in severe sepsis
- clinical definitions of SIRS, sepsis and severe sepsis are not sufficiently precise
- a failure to adequately power sepsis trials

(64).

For these reasons, there has historically been little success in the development of an adequate broad-spectrum treatment for severe septicemia. Treatments thus far have consisted of antimicrobial drugs, cytokine antagonists (96), intensive insulin therapy (86,87) and administration of recombinant human activated protein C (10), with cytokine antagonists alone being the least successful (96). Antimicrobial drugs are necessary but not sufficient for the treatment of sepsis. Ironically, antimicrobial drugs may actually precipitate septic changes by liberating antimicrobial products (62).

Sepsis profoundly alters systemic hemodynamics and metabolism. Early sepsis is characterized by a hypermetabolic phase consisting of a pattern of increased cardiac output, decreased systemic vascular resistance, and a redistribution of organ blood flow. These responses are associated with elevations of circulating insulin and counterregulatory hormones and the release of inflammatory mediators (18). Intensive insulin therapy has been shown to be promising in that the incidence of bacteremia and sepsis is significantly reduced with the utilization of insulin (87). More recent studies involving intensive insulin therapy would indicate the beneficial effects seen with an insulin regimen might be more a function of control of hyperglycemia than direct effects of the insulin itself (86).

Regardless, recombinant human activated protein C is the only current treatment for sepsis recognized by the Food and Drug Administration. Recombinant human activated protein C has the benefit of providing anti-inflammatory, antithromobotic and profibrinolytic properties. All of these properties prove to be essential in efficient recovery from an endotoxic insult.

The Metabolic Response to Endotoxin

Initially, patients with septicemia experience an increase in the mobilization and utilization of glucose in conjunction with a major influx of immunologic factors. One important feature of the hypermetabolic response *in vivo* is an increase in the synthesis and release of glucose from the liver early in an endotoxin challenge (46). This leads to a brief state of hyperglycemia coupled with elevated insulin levels (20,54,95). This increase in glucose appears to be unaffected by the elevation in insulin secretion. A state of insulin resistance develops in the presence of conditions favorable for gluconeogenesis. These conditions are characterized by lactic acidemia, increased plasma amino acids and increased levels of glucogenic hormones (18,22,36). The resistance to the effects of insulin is likely a result of not only the sustained high output of glucose by the liver but also in decreased insulin-stimulated utilization of glucose by muscle and other peripheral tissues (20).

Endotoxemia can be divided into two categories with two different series of metabolic outcomes. The first category, low dose endotoxemia, is more experimental in nature and has less clinical relevance. Low dose endotoxemia is considered important, as it is a means to study the metabolic intermediates between the states of health and high

dose endotoxemia. This condition displays a transient hyperglycemia that is a result of the increased rate of glucose production that exceeds the enhanced glucose utilization by peripheral tissues (45). The circulating glucose level gradually returns to basal values without ever falling to a hypoglycemic level. It is thought that the elevated circulating levels of catabolic hormones and increased gluconeogenic precursor availability are responsible for the maintenance of hepatic glucose production and supply of glucose to sustain the increased demands of peripheral tissues (45).

The second category, high dose endotoxemia, is more clinically relevant and is often recapitulated in animal models as a means to better understand the metabolic and immunologic complexity of this condition. Like low dose endotoxemia, this condition displays a transient hyperglycemia early in infection, although it can produce a severe hypoglycemia that appears to result primarily from a subsequent reduction in hepatic glucose production (44). This results from the depletion of hepatic glycogen reserves and later impairment in the gluconeogenic capacity and hormonal responsiveness in the liver (44). Throughout a four-hour period, rates of glucose production, glucose recycling, and glucose clearance become elevated and typically remain elevated long after early hyperglycemia (78). Studies conducted in rats by Lang *et al.* (44) and Buday *et al.* (16) have shown that when given a bolus of LPS, rats had a dramatic increase in early glucose concentration and, by the end of the study, had an increase in all other parameters measured with the exception of insulin, hepatic glycogen and muscle glycogen (Table 1).

Table 1: Metabolic and Hormonal Alterations Induced by *E. coli* Endotoxin.

Analyte	% change over basal
Glucose at 1 h	+69%
Glucose at 4 h	+19%
Lactate at 4 h	+86%
Insulin at 4 h	-29%
Glucagon at 4 h	+340%
Norepinephrine at 4 h	+750%
Epinephrine at 1 h	+3300%
Epinephrine at 4 h	+2500%
Corticosterone at 4 h	+300%

Metabolic Parameter	% change over basal
R_a at 1 h	+70%
R_a at 4 h	+28%
Glucose Recycling at 4 h	+290%
Glucose Clearance at 4 h	+17%
Liver Glycogen* at 4 h	-86%
Muscle Glycogen* 4 h	-27%

Table adapted from data collected by Lang *et al.* (44) and Buday *et al.* (16). Glycogen data (*) has been obtained from Buday *et al.*, all other data is from Lang *et al.*. R_a is endogenous glucose production.

The increased rate of production represents primarily the early increased rate of gluconeogenesis. Although there is a relatively prolonged increase in glucose production in the early phase of endotoxemia, this increase is not sustained but instead is followed by a hypoglycemic phase characterized by a depression in gluconeogenesis (47). The increased rate of glucose carbon recycling indicates an accelerated peripheral conversion of glucose to lactate, and subsequent conversion to glucose via hepatic gluconeogenesis is driven in part by the rising arterial lactate concentration (78). Gluconeogenesis is increased *in vivo* in spite of a decrease in the gluconeogenic rate-limiting enzyme PEPCK (47). Previous studies suggest that the elevated gluconeogenesis observed during the early hyperglycemic phase is associated with increases in both glucose-6-phosphatase

mRNA levels and enzymatic activity (48) whereas glucose-6-phosphatase activity is decreased during the hypoglycemic phase of endotoxemia (6).

It has been observed that primary gluconeogenic enzymes such as phosphoenolpyruvate carboxykinase (PEPCK) (25), glucose-6-phosphatase and fructose-1,6-diphosphatase (53) are greatly reduced during infection. Fructose-2,6-biphosphate is the most potent regulator of gluconeogenesis and is rapidly accumulated early in infection. The outcome is the eventual stimulation of phosphofructo-kinase activity leading to the preferential shunting of hexoses through the glycolysis pathway rather than toward the gluconeogenic pathway later in infection (5). The resulting consequence can be hypoglycemia as a result of a depleted glucose reserves. Conversely, it has been observed that rates of gluconeogenesis are greatly depressed in isolated perfused livers obtained from septic rats when substrate delivery and hormonal stimulation are standardized to sham livers (21). Studies using lactate as a substrate for gluconeogenesis showed lactate dependent increases in glucose production declined by 50% in perfused livers obtained from septic rats (21). The actual mechanism by which endotoxin interferes with gluconeogenesis is still unknown. The differences in gluconeogenesis observed in septic *in vivo* and *ex vivo* liver studies may be attributed to differences in liver damage caused by endotoxic insult. Although variations between models are apparent, the isolated perfused liver model has an important role in studying the primary effects of endotoxemia, as this model is void of the interference of the cardiovascular system, the nervous system, the adrenal glands, and other tissues. Regardless, the *in vivo* system remains our model of choice due to the functioning completeness of the whole body system.

The muscle response to endotoxin has been studied extensively in regards to glycogen content and the increased delivery of gluconeogenic substrate during sepsis (19,22). Early studies have shown that when challenged with ^{51}Cr –labeled *E.coli* endotoxin, the muscle contained no more than ~1% of the total radioactivity (15). This observation suggests that glycogen changes in the muscle are secondary to those of liver glycogen changes due to the distribution of the endotoxin. It has been previously observed that endotoxemia triggers a rapid depletion in skeletal muscle glycogen content (33), although skeletal muscle glucose uptake and skeletal muscle glucose clearance is increased following a bolus of LPS (69,71). Buday *et al.* have shown that endotoxemic rats had 27% less glycogen in skeletal muscle and 86% less glycogen in the liver four-hours after a bolus of endotoxin compared to basal (16). This is thought to be associated with an increased phosphorylase a in both tissues compared to controls (16). Glycogen repletion studies also demonstrated skeletal muscle was able to synthesize glycogen at similar rates when rats were infused with either saline or glucose following a four-hour endotoxemia study, whereas hepatic glycogen synthesis was reduced in rats infused with saline vs. the rats infused with glucose (16).

Little is known about the effects of glucagon on the response to endotoxin *in vivo,* although the likely hormonal effectors responsible for the fall in glycogen content are the elevated plasma concentrations of catecholamines and glucagon. In studies where endotoxin treated rats were maintained either hypoglycemic or euglycemic with an infusion of glucose, glucagon remained elevated (increased by 24 fold and 9 fold; respectively) and insulin levels remained decreased (decreased 83% and 58%; respectively) (44).

Other factors such as adrenal cortical hormones and protein C have been shown to play a role in the metabolic disequilibrium associated with endotoxemia. Cortisone promotes glyconeogenesis and a negative nitrogen balance. Early studies by Berry *et al.* showed that mice exposed to a lethal dose of endotoxin and then given a subcutaneous injection of 5 mg cortisone had an increase of 70% on average in survival rate over mice with a lethal dose alone (11). Mice that survived a lethal dose of endotoxin in conjunction with the administration of cortisone had greater carbohydrate reserves than the mice with endotoxin challenge alone. The survival rate associated with cortisone injection appears to be related to the ability of cortisone to allow for the favorable quantity of carbohydrate reserves remaining to sustain life. The overall positive outcome of cortisone treatment during endotoxemia may also be associated with the anti-inflammatory effects of this group of steroids (11).

The Neuroendocrine Response to Endotoxin

There has been much controversy as to the specific role of epinephrine and norepinephrine in the response to an endotoxin challenge. This controversy is due in part to the great differences observed to the response between animal and human models of sepsis. It is thought that the catecholamine response to endotoxemia is similar in magnitude to the glucagon response, yet both have been hotly debated. One fact remains constant across all experimental models- glycogenolysis is increased during sepsis primarily through the conversion of the inactive form of phosphorylase to the active form. In large part, catecholamines, prostaglandin, and glucagon are responsible for this conversion (17). The effects of catecholamines are wide ranging. An intravenous bolus

of endotoxin decreases cardiac output in a dose dependent manner. Although cardiac output is decreased, adrenal and hepatic arterial blood flows are markedly increased in guinea pigs (28). This is important when taking into account the enhanced hepatic gluconeogenic rate and increased catecholamine and corticosterone synthesis by the adrenal glands during endotoxemia. Conversely, the infusion of epinephrine in animals causes increased glucose turnover, gluconeogenesis, lactic acidemia, and transitory hyperglycemia, which are all hallmarks of endotoxemia (78). Studies utilizing combined α- and β- adrenergic blockade by phentolamine and propranolol prevented the early transient hyperglycemia normally observed following an LPS bolus and either prevented or considerably attenuated the early increases in tissue glucose utilization (58). The early increase in glucose uptake may be mainly attributed to adrenergic stimulation and the resultant hyperglycemia, while sustained elevation may be due to mechanisms independent of hyperglycemia (58). Similar studies have also shown combined α- and β-adrenergic blockade completely prevents LPS induced increases in glucose production and glucose recycling, but blunts an increase in plasma lactate concentration and does not increase glucose clearance (78). Combined adrenergic blockade also completely prevented the LPS induced increase in liver glucose uptake while there was a significant reduction in the spleen, intestine, skin, fat, and gastrocnemius (58). Although glucagon is a vital metabolic hormone, it is interesting to note that, in rat studies that used a combined α- and β- adrenergic blockade, plasma glucagon concentrations were similarly elevated as in endotoxemic control rats, although the changes in carbohydrate metabolism were eliminated (78).

The Immune Response to Endotoxin

Serum proteins bind endotoxin, lead to the modification of endotoxic properties, and potentially induce detoxification in some circumstances. It has also been established that small amounts of serum can enhance endotoxin binding and subsequent activation of cells. The effects observed in endotoxin binding are related to a unique serum protein lipopolysaccharide-binding protein (LBP) (80). LBP is a 60 kd serum glycoprotein that is synthesized in the hepatocytes of several species to include humans, mice, and rats (82). LBP binds with high affinity to the lipid A portion of endotoxin causing the resulting complex to bind to either membrane bound CD14 (mCD14) or soluble CD14 (sCD14) (82). The endotoxin:LBP:mCD14 complex activates macrophages whereas the endotoxin:LBP:sCD14 complex reacts with endothelial and epithelial cells, leading to their activation and subsequent expression of cytokines and adhesion molecules (68). The liver is an important source of both LBP and sCD14 and thus plays a vital role in the clearing of endotoxin.

One of the consequences of endotoxin exposure is the circulating number of polymorphonuclear neutrophils (PMNs) is rapidly reduced and there is a subsequent sequestration of PMNs into the liver. A state of neutropenia develops due to the rate of PMN removal from the circulation being greater than the increased rate of neutrophil entry into the blood (32). The magnitude and duration of the neutropenia is dependent on the severity of the insult (43). PMN accumulation in the liver adds a new group of nonparenchymal cells and is believed to occur as the result of chemotactic signals released by Kupffer cells (56,97). The preferential localization of neutrophils is possibly related to the high rate of LPS clearance and rich population of macrophages within the

liver (52). Stimulated PMNs actively secrete potent oxygen-derived radicals and destructive enzymes (defensins, lysozyme, collagenase, and lactoferrin) that can cause severe liver damage, which may contribute to the development of hepatic liver failure observed during severe sepsis (27). It is believed that the specific chemotactic agents responsible for the induction and migration of PMNs are the C5a component of complement and leukotriene B4 (LTB4), although there is new evidence that TNF-α may also be a chemotactic candidate (73). This is important because neutrophil adhesion plays an essential role in the progression of inflammation. Hepatic injury may result from the increase in complement and TNF-α as these factors contribute to the upregulation of adhesion molecules on neutrophils (94). Attempts have been made to eliminate neutrophils from the blood by using antibodies against the neturophils. It has been observed that antibody-coated neutrophils disappear from the blood and accumulate mainly in the liver where they become functionally impaired and eliminated by resident macrophages (9). Neutrophils may also pose a threat to liver tissue by becoming trapped in sinusoids due to the slightly smaller diameter of sinusoids compared to neutrophils. This may be exacerbated by the fact that endotoxin activation causes swelling of endothelial cells and Kupffer cells, which further decreases sinusoidal diameter.

Both pro- and anti-inflammatory cytokines are upregulated during endotoxemia. Cytokines are generally released and act at the site of endotoxin insult but cytokine levels are elevated in the circulation and cytokines may be recruited to the area via chemotactic signaling. TNF-α is typically the first cytokine to appear in the circulation after endotoxin challenge and typically peaks after 90 minutes (35). There is a tight correlation between the magnitude of bacterial challenge and the extent of endotoxin

release. The release of TNF-α is shortly followed by other proinflammatory cytokines including IL-1β, IL-6, IL-12 and IFN-γ (14). The initial peak of TNF-α also triggers the release of several anti-inflammatory cytokines to include IL-10, IL-1ra, and soluble TNF-α receptors (14). During sepsis, the circulating concentrations of soluble TNF-α receptors and the naturally occurring IL-1 inhibitors, soluble IL-1 receptor type II and IL-1ra, are increased substantially (89). This increase may provide a means for the host to limit systemic TNF-α and IL-1β toxicity.

During endotoxemia, circulating TNF-α, IL-1β, IL-6, epidermal growth factor, insulin-like growth factor, and fibroblast growth factor are cleared by the liver (2). Up to 30% of TNF-α is recovered in the liver within 15 minutes (the half-life of TNF-α) after intravenous injection. IL-1β mRNA is greatly increased within 1-2 hours whereas the IL-1 receptor antagonist (IL-1ra) mRNA peaks 2-4 hours following intravenous endotoxin challenge (85). Although the half-life for IL-1β is 4 hours, it begins to collect in the liver within 20 minutes following endotoxin injection (39). TNF-α and IL-β can induce the expression of IL-6 mRNA and an increase in IL-6 is generally detectable within 1 hour after endotoxin exposure. IL-6 has a relatively short half-life of 1.5-3 minutes and up to 80% of radiolabeled IL-6 from a single intravenous injection can be detected in the liver within 20 minutes (77). The liver plays an important role in the inflammatory response to endotoxin but a striking caveat is that the liver may actually limit the beneficial systemic effects of these cytokines by clearing them prematurely.

The Role of Cytokines in Response to Endotoxin

TNF-α and IL-1β share an extraordinary array of biological effects. The systemic inflammatory effects of TNF-α include the induction of the cytokine network, the coagulation system, fibrinolysis, and neutrophils (88,90). All of these are important in the regulation of the inflammatory response associated with sepsis. IL-1β has been shown to induce similar effects without the activation of neutrophils. It has been demonstrated that administration of high doses of either TNF-α or IL-1β to laboratory animals reproduces many characteristics observed in sepsis (63,83). During sepsis, approximately 50% of radiolabeled endotoxin will accumulate in the liver within five minutes after an intravenous injection and the main site of accumulation is the Kupffer cells (52). Rat Kupffer cells exposed to endotoxin produce TNF-α, and the addition of interferon-γ (IFN-γ) enhances the production of TNF-α (24). If left unchecked, together IL-1β and TNF-α in excess can result in synergistic toxicity and have a lethal effect. It is also important to note the cytokines TNF-α and IL-1β are responsible for most of the humoral modifications observed after endotoxin challenge (91).

Glucose uptake is increased in the liver immediately following an endotoxin challenge. Prior to endotoxin challenge, the Kupffer cells account for 25% of total hepatic glucose uptake in normal livers (67). It is has been observed that glucose uptake is increased in macrophages and endothelial cells and remains constant in parenchymal cells immediately following an endotoxin insult (56). Interestingly, TNF-α stimulates the same effect, leading one to speculate that this cytokine may play a crucial role in alterations in glucose uptake. Experimental infusion of TNF-α increases glucose production without significantly increasing blood lactate concentration or causing a

hemodynamic response (7). TNF-α infusion also increases plasma insulin, glucagon, and catecholamine concentrations (7) and increases glucose uptake in the liver, spleen, intestine, skin, and lung (57). Thus, it is likely that cytokine release following endotoxin exposure may be one of the mechanisms by which endotoxin exerts its effects on glucose metabolism (57). The hepatic immune response, IL-1β and TNF-α released by macrophages, is controlled by an increase in glucose uptake in Kupffer cells and is critical in the hepatic antibacterial defense against infection. Alterations in any step of this process may have detrimental effects on the efficiency of the body to properly clear endotoxin.

Early release of TNF-α appears to be essential in the role of the induction of both pro-and anti-inflammatory cytokines. This has been demonstrated in experiments where anti-TNF-α antibodies given prior to endotoxin challenge blocks the increase in plasma and serum concentrations of IL-1β, IL-1ra, IL-6, IL-10, and soluble TNF-α receptors (12). Unfortunately, this treatment is not realistic for the clinical setting as anti-TNF-α treatment is only protective against lethality when given before, simultaneously, or within 30 minutes after a lethal dose of endotoxin exposure.

Conversely, the anti-inflammatory cytokine IL-10 appears to have a protective function in models of endotoxemia. Typically, anti-inflammatory cytokines inhibit the inflammatory process by aiding in the reduction of proinflammatory cytokine production. This has been shown in studies where recombinant IL-10 was injected directly prior to injecting mice with a lethal dose (LD_{100}) of endotoxin. The IL-10 injection markedly reduced TNF-α release and prevented lethality (30). In humans, recombinant human IL-10 has been observed to attenuate plasma TNF-α, IL-6, and IL-8 levels, the rise in body

temperature, and activation of the fibrinolytic system and coagulation system (65,66). The suppression of IL-10 by neutralization in septic mice results in an increase in the production of proinflammatory cytokines, including IFN-γ and TNF-α, and leads to death (49). Similar results are also observed in IL-10 knockout mice exposed to endotoxin. These mice have increased mortality after endotoxin injection and elevated levels of TNF-α, IL-1β, IL-6, IL-12, and IFN-γ (44). IL-10 proves to be an important part of the autoregulatory mechanism associated with controlling the production of proinflammatory cytokines and endotoxin associated toxicity *in vivo*.

The Role of Interleukin-6 in Inflammation and Metabolism

IL-6 is found in the body as intracellular protein and circulating protein. Physiological stimuli for the synthesis of IL6 are IL-1, TNF, PDGF, oncostatin M, and bacterial endotoxin. IL6 is also produced in the anterior lobe of the pituitary and can be induced by endotoxin and all substances responsible for elevating intracellular levels of cAMP. The rate that IL-6 mRNA can be transcribed is affected by multiple transcription factors including Nf-κB. The resulting IL-6 protein product can work in three ways: 1) in an autocrine manner whereby IL-6 can enhance the regulation of IL-6 in the infected local area, 2) in a paracrine manner whereby IL-6 can contribute to the inflammatory process in surrounding tissues, and 3) in an endocrine manner whereby IL-6 can send extracellular feedback messages to the brain and other organs via circulation through the blood stream. Following a bolus of endotoxin, IL-6 protein enters the circulation and peaks within 60 minutes (29). Major sites of IL-6 protein release are macrophage-rich tissues, such as the liver and spleen, and skeletal muscle and circulating IL-6 can be

elevated up to 300 fold during endotoxic insult (29,51). IL-6 actions are mediated through binding with high affinity either to gp130 (a common form of cytokine signal transducer) membrane bound IL-6 receptors or to soluble IL-6 receptors. The binding of IL-6 protein to either IL-6 receptor type leads to the formation of a gp130/gp130 homodimer complex that in turn activates IL-6 signal transduction. The soluble IL-6 receptor is unique from other soluble cytokine receptors in that it serves an agonistic function once bound to IL-6 protein, allowing cells that lack a membrane bound IL-6 receptor to be responsive to IL-6 (38). IL-6 is responsible for a wide array of biological activities to include immunoglobulin production, proliferation and differentiation of T cells, enhancement of natural killer cell activities, maturation of megakaryocytes, and induction of acute-phase protein synthesis (38).

The acute phase response in the liver is regulated by cytokines, glucocorticoids, and nitric oxide. The primary cytokines that have been shown to be involved in this regulation are IL-1β (60), TNF-α (75), and IL-6 (34). Neither TNF-α nor IL-1β is capable of regulating a complete acute response, although adequate regulation can be accomplished indirectly by TNF-α in the presence of glucocorticoids or IL-6 (8). On the contrary, IL-6 is the most important cytokine with regard to the acute phase response as it is the only cytokine capable of inducing an almost complete response (34). It is possible circulating IL-6 and IL-6 derived from peripheral macrophages, Kupffer cells, and hepatocytes are responsible for the acute response. Regardless, IL-6 requires the presence of glucocorticoids to achieve the maximal and complete acute phase response. IL-6 regulates the acute-phase protein response by stimulating hepatocytes to produce

acute phase reactants such as C-reactive protein, serum amyloid A, α1-acid glycoprotein, α1-antitrypsin, and fibrinogen.

IL-6 is most commonly recognized as a proinflammatory cytokine due to its role during exaggerated inflammatory states such as severe sepsis and type II diabetes. Nearly all published clinical studies involving severe sepsis and cytokine levels have found a positive correlation between IL-6 concentrations on admission and mortality (64). Although IL-6 is typically considered a proinflammatory cytokine, it has anti-inflammatory properties as well, making this cytokine unique. Multiple studies have been conducted to elucidate the role of IL-6 has in mediating hormonal and immunological changes both *in vivo* and *in vitro.* In clinical studies, intravenously infused IL-6 produces mild clinical symptoms such as fever and chills, but it is not nearly as toxic as TNF-α and IL-1β. The anti-inflammatory effects of IL-6 are demonstrated by its ability to inhibit endotoxin-induced TNF-α and IL-1β production by mononuclear cells *in vitro* and to reduce TNF-α release in endotoxemic mice *in vivo* (1). IL-6 has also been shown to induce an increase in plasma levels of naturally occurring inhibitors of TNF-α and IL-1β in the form of soluble TNF-α receptor type I and IL-1ra (81).

Metabolic studies conducted *in vitro* using HepG2 cells and primary mouse hepatocytes that were acutely pretreated with IL-6 demonstrate impaired insulin receptor signaling as well as impaired insulin-dependent glycogen synthesis (74). *In vivo* studies using a short-term infusion of IL-6 in humans have shown increases in circulating free fatty acids, and the increase in IL-6 may inhibit the negative effects of TNF-α, thus indirectly promoting glucose uptake and enhancing insulin sensitivity in peripheral tissues (29). A bolus injection of IL-6 in rats has been shown to produce a transient

increase in plasma glucagon and increase plasma glucose and insulin levels after 90 minutes, and it is believed that the increase in the plasma insulin level was due to the increase in glucose and not the IL-6 (79). Similarly, fasting glucose levels were increased in a dose dependent manner in healthy human subjects within 60 minutes following a bolus of IL-6 (84). Glucagon levels increased significantly and peaked between 120 to 150 minutes following the IL-6 bolus (84). Chronic IL-6 infusion reduces hepatic insulin autophosphorylation and tyrosine phosphorylation of both insulin receptor substrates-1 and -2 (40). In these studies, insulin tolerance tests revealed reduced insulin sensitivity, yet the chronic infusion of IL-6 failed to suppress skeletal muscle insulin receptor signal transduction, suggesting that chronically elevated IL-6 selectively impairs hepatic insulin signaling *in vivo.* Likewise, it has been observed that IL-6 blockade by anti-IL-6 antibodies can be protective in sepsis (70). The administration of anti-IL-6 antibodies shortly after the initiation of cecal ligation and puncture inhibits C5a receptor mRNA expression during the onset of sepsis and significantly improves survival (70).

As one might expect, the unique pro- and anti-inflammatory nature of IL-6 adds many layers of complexity to discerning its role in a pathogenic state such as sepsis. There is a profound lack of data correlating the interaction of increased levels of IL-6 during sepsis with alterations in carbohydrate metabolism. Current studies have only begun to touch the tip of the iceberg.

CHAPTER II

MATERIALS AND METHODS

Animal Care and Husbandry

All procedures were approved by the Vanderbilt University Animal Care and Use Committee and followed NIH guidelines for the care and use of laboratory animals. All experiments were performed on mice with the C57BL/6J background between four and five months of age. Mice were weaned at three weeks of age and separated by sex. Mice were identified by ear punching, and a tail biopsy was taken with the purpose of obtaining a genomic DNA sample. Genotyping was performed by polymerase chain reaction (PCR) on DNA isolated by a DNeasy Tissue Kit (Qiagen, Valencia, CA). PCR primer sequences used for the genetic models were obtained from Jackson Laboratories. Mice were housed in an environment with five mice per micro-isolator cage. Mice were maintained on a light cycle of 0700-1900 at 23°C and were allowed free access to Purina 5001 laboratory rodent chow diet and water.

Mouse Models

Interleukin-6 knockout mice have no interleukin-6 mRNA and protein expression (41). Mouse models with both the presence and absence of IL-6 mRNA and protein expression were utilized for all experiments. IL-6 knockout mice ($IL\text{-}6^{-/-}$) on a C57BL/6 background (Jackson Laboratories, Bar Harbor, ME) were bred to C57BL/6J mice (Jackson Laboratories, Bar Harbor, ME) to yield heterozygous pups ($IL\text{-}6^{+/-}$). Male and

female IL-$6^{+/-}$ mice were bred to generate Mendellian litters. IL-$6^{-/-}$, IL-$6^{+/-}$ and IL-$6^{+/+}$ genotypes were confirmed by PCR utilizing primer sequences obtained from JAX (Jackson Laboratories, Bar Harbor, ME) in accordance with original forward, reverse and NEO primers originally published by *Kopf et al.* (41). Mice of both genders were utilized for all studies. IL-$6^{+/-}$ mice were used to continue breeding schemes mentioned above.

Surgical Procedures

Mice were anesthetized with an intraperitoneal injection of pentobarbital (70mg/kg body weight). Following administration of anesthesia, the skin on the interscapula and on the right and left sides of the neck was shaved and sterilized with 10% povidone-iodine. Surgery was initiated with loss of foot withdrawal and corneal blinking reflex.

The left common carotid artery was catheterized for the sampling of well-mixed arterial blood with a two-part catheter consisting of modified PE-10 tubing (inserted into the artery) connected to silastic tubing (0.025 in OD). The PE-10 was stretched by heating under sterile water and then quickly chilled in order to decrease the diameter. The PE-10 was then inserted approximately 2mm into the silastic tubing and beveled at 45° on the exposed end. A small skin incision (~5mm) was made approximately 3mm adjacent to the trachea. The common carotid artery was isolated and separated from the vagus nerve and surrounding muscle. Two thin threads of silk (6-0 Silk, Davis+Geck, Wayne, NJ) were passed under the artery. The cephalic thread was tied to prevent bleeding and then the artery was clamped with a small bulldog clamp. A small incision was made just below the ligature and the catheter was inserted into the lumen. The

modified PE-10 was inserted approximately 9mm into the left common carotid artery such that the catheter tip was near the aortic arch. The catheter was fixed with a second thread and the thread previously used to prevent bleeding in order to secure the catheter in place. The bulldog clamp was removed to verify the proper function of the catheter.

The right jugular vein was catheterized for infusions with a silastic catheter (0.025 in OD). A small longitudinal incision (~5mm) was made in the skin just over the location where the anterior jugular, acromiodeltoid, and cephalic veins join. The connective tissues surrounding this junction were carefully removed. Two thin threads of silk (6-0 Silk, Davis+Geck, Wayne, NJ) were passed under the jugular vein below the level of the junction and separated by about 3 mm. The cephalic thread was placed just below the joint and was tied to prevent bleeding. A small incision was then made just below the ligature and the catheter was inserted into the lumen and advanced ~13 mm. The catheter was secured with the second thread and with the free ends of the cephalic thread were used to anchor the catheter in place.

The free ends of the catheters were tunneled under the skin to the back of the neck with a blunt 16 gauge needle, where the loose ends of the catheters were attached via stainless steel connectors to tubing made of Micro-Renathane (0.033 in OD), which were exteriorized and sealed with stainless steel plugs. Mice were moved to a warming bed following surgery and were observed until they were fully awake. Both lines were flushed daily with ~50 µl of saline containing 200 U/ml of heparin and 5 mg/ml of ampicillin. Animals were individually housed after surgery and body weight was recorded daily.

In Vivo Metabolic Experiments

All metabolic experiments were performed following a ~7 day postoperative recovery period. The recovery period was deemed sufficient when body weight was restored within 10% of pre-surgery body weight. On the day of the study conscious, unrestrained mice were placed in ~1 L plastic container lined with bedding and fasted for 5 h. Approximately 2 h prior to an experiment, Micro-Renathane (0.033 in OD) tubing was connected to the catheter leads and infusion syringes. A 5 μCi (100 μL) bolus of 3-[^{3}H]-D-glucose was given followed by a constant infusion at a rate of 0.05 μCi/min (NEN, #NET331C; 1 uL/min). Approximately 1 h prior to an experiment, red blood cells from a donor mouse on a C57Bl/6J background were washed with 0.9% heparinized saline and infused at a rate of 2 μl/min for the duration of the study to minimize the fall in the hematocrit (<5%)). Following the 2 h equilibrium period, a baseline arterial blood sample (230 μl) was drawn for the measurement of arterial blood glucose, 3-[^{3}H]-D-glucose, hematocrit, plasma insulin, plasma glucagon, catecholamines and cytokines.

LPS Experiments in IL-6$^{-/-}$, IL-6$^{+/-}$, and IL-6$^{+/+}$ Mice

The maximum effects of IL-6 during an LPS challenge can be observed between 180 and 360 min (29,77). For this reason, the current study design assesses the effect of LPS over a time period of 265 min (Figure 1). Approximately 5 min following the baseline arterial blood sampling, mice were given a 250 μg/mouse bolus of *E.coli* (serotype 0111:B5) endotoxin (Sigma, St. Louis, MO) followed by 25μL saline and the clock was reset (t = 0 min) (Figure 3a). At t = 30 min, arterial blood (~230 μL) was sampled in order to determine arterial blood glucose, 3-[^{3}H]-D-glucose, hematocrit,

plasma insulin, plasma glucagon, catecholamines and cytokines. At t = 60 and 120 min, arterial blood (~10 μL) was sampled in order to assess the arterial blood glucose concentration. At t = 180 and 240 min, arterial blood (~70 μL) was sampled in order to determine arterial blood glucose, 3-[^{3}H]-D-glucose, and cytokine levels. And at t = 210 min, arterial blood (~30 μL) was sampled in order to determine arterial blood glucose and 3-[^{3}H]-D-glucose concentrations.

Shortly after the t = 240 sampling, a 13 μCi bolus of 2-deoxy[^{14}C]glucose ([2-^{14}C]DG) was administered in order to determine R_g and the clock was reset. Arterial blood (~30 μL) was sampled to assess blood glucose and plasma 3-[^{3}H]-D-glucose and [2-^{14}C]DG concentration 2, 5, 10, and 15 min after the bolus was given. At 25 min after the bolus (t = 265 for length of study), a final arterial blood sample (~230 μL) was taken and processed in the same manner as the baseline blood sample with the addition of the determination of plasma [2-^{14}C]DG. Following the last arterial blood sample, mice were anesthetized and the soleus, gastrocnemius, superficial vastus lateralis (SVL), omental adipose tissue, liver, kidney, duodenum, jejunum, diaphragm, heart, subcutaneous adipose tissue and brain were excised, immediately frozen in liquid nitrogen, and stored at -70°C until future tissue analysis.

LPS Experiments with Replacement of Interleukin-6 in IL-6$^{-/-}$ Mice

For LPS experiments the interleukin-6 replacement in IL-6$^{-/-}$ mice, studies were carried out exactly the same as the previous LPS studies with the following exceptions (Figure 2). Approximately 5 min following the baseline arterial blood sampling, IL-6$^{-/-}$ mice were given a 250 μg/mouse bolus of *E.coli* (serotype 0111:B5) endotoxin followed

by 25μL saline. Immediately following the bolus of endotoxin, a constant infusion of rmIL-6 (16 μg/hr) (Research Diagnostics, Inc., Flanders, NJ) at a rate of 1 μL/min was started and the clock was reset (t = 0 min) (Figure 3b). At t = 30 min, arterial blood (~230 μL) was sampled in order to determine arterial blood glucose, 3-[^{3}H]-D-glucose, hematocrit, plasma insulin, plasma glucagon, catecholamines and cytokines. Immediately following the t = 30 arterial blood sample, the pump rate of the rmIL-6 was increased to 2 μL/min in order to simulate the natural IL-6 response observed in wild type animals. At t = 60 and 120 min, arterial blood (~10 μL) was sampled in order to assess the arterial blood glucose concentration. At t = 180 and 240 min, arterial blood (~70 μL) was sampled in order to determine arterial blood glucose, 3-[^{3}H]-D-glucose, and cytokine levels. At t = 210 min, arterial blood (~30 μL) was sampled in order to determine arterial blood glucose and 3-[^{3}H]-D-glucose concentrations.

Processing of Plasma and Muscle Samples

Blood Glucose Concentration

Whole blood glucose concentration was measured on arterial blood samples during all metabolic studies at the time points indicated in figures 1 and 2. For determining blood glucose concentration, ~10 μL of arterial blood was collected into a HemoCue B-Glucose Microcuvette and measured on a HemoCue B-Glucose Analyzer (HemoCue, Mission Viejo, CA). The HemoCue Analyzer used in these studies was calibrated daily using the standardized control Microcuvette provided with the analyzer. The theory of this assay is based on two concepts, hemolysis and a glucose reaction.

Saponin in the cuvette lyses the erythrocytes and partially dissolves the membranes. The following is a depiction of the reactions used to determine the glucose concentration:

$$\alpha\text{-D-glucose} \xrightarrow{\text{mutarotase}} \beta\text{-D-glucose}$$

$$\beta\text{-D-glucose} + \text{NAD} \xrightarrow{\text{glucose dehydrogenase}} \text{D-gluconolactone} + \text{NADH}$$

$$\text{MTT} \xrightarrow{\text{diaphorase + NADH}} \text{formazan}$$

whereas MTT is the tetrazolium salt 3-[4,5-dimethylthiazol-2yl-]-2,5-diphenyltetrazolium bromide. Formazan is measured spectrophotometrically at 660 and 840 nm.

Plasma Immunoreactive Insulin

Immunoreactive insulin was measured on the baseline plasma sample as well as on plasma samples obtained at t = 30 and 265 min in all metabolic experiments. The assay uses a Linco Rat Insulin Radioimmunoassay (RIA) kit (Linco Research, Inc., St. Charles, MO) and a double antibody method (59). 50 μL plasma samples are incubated with ^{125}I-rat insulin and a guinea pig anti-rat insulin primary antibody that equally cross reacts with mouse and porcine insulin. The labeled and unlabeled insulin compete for the limited number of antibody binding sites. If the amount of unlabeled insulin is increased, there will be a decrease in the amount of labeled insulin binding to the antibody. Insulin bound by the primary antibody was precipitated with a secondary antibody. Following centrifugation and decanting, pellets were counted in a Cobra II Auto-Gamma counter (Packard Instrument Co., Downers Grove, IL). The insulin concentration in the sample

was inversely proportional to the radioactivity in the pellet. Insulin concentrations were determined using a standard curve generated from known concentrations of insulin and resultant radioactivities. Samples were corrected for non-specific binding. Controls consisted of two commercial and four in-house controls for each RIA.

Plasma Glucagon

Immunoreactive glucagon was measured on the baseline plasma sample as well as on plasma samples obtained at t = 30 and 265 min in all metabolic experiments. The assay uses a Linco Rat glucagon (RIA) kit (Linco Research, Inc., St. Charles, MO) and a double antibody method (61). 50 μL plasma samples are incubated with ^{125}I-rat glucagon and a guinea pig anti-rat glucagon primary antibody that equally cross reacts with mouse, rat, rabbit, hamster, pig, cow, camel, monkey and human glucagon. The labeled and unlabeled glucagon compete for the limited number of antibody binding sites. If the amount of unlabeled glucagon is increased, there will be a decrease in the amount of labeled glucagon binding to the antibody. Glucagon bound by the primary antibody was precipitated with a secondary antibody. Following centrifugation and decanting, pellets were counted in a Cobra II Auto-Gamma counter (Packard Instrument Co., Downers Grove, IL). The glucagon concentration in the sample was inversely proportional to the radioactivity in the pellet. Glucagon concentrations were determined using a standard curve generated from known concentrations of glucagon and resultant radioactivities. Samples were corrected for non-specific binding. Controls consisted of two commercial and four in-house controls for each RIA.

Epinephrine and Norepinephrine

Plasma epinephrine and norepinephrine content was assessed by high performance liquid chromatography with electrochemical detection (HPLC/EC) (31) after alumina extraction (4), elution and pre-concentration. 50 μL of glutathione and EDTA preserved plasma was absorbed onto alumina at a basic pH of 8.6. The solution was shaken and centrifuged and the supernatant was removed. The alumina pellet was then rinsed with three deionized-water washings to remove contaminants. The catecholamines were then eluted from the alumina with 0.1M perchloric acid (PCA), the samples were centrifuged and the supernatant was again rinsed with PCA.

The samples were injected onto a HR-80, reverse phase, 3 μm octadecylisilane column and run on the Coulochem II (ESA, Bedford, MA) electrochemical detector. Potentials were optimized by exposure to an electric field. Recovery was calculated from the ratio of 2,3-dihydroxybenzoic acid (DHBA) and standard peak heights in the injection. A standard curve from known concentrations was utilized for each hormone.

Plasma Cytokine Concentration

Cytokines were analyzed for all metabolic experiments using the bead-based multiplexing Luminex xMAP technology (Luminex, Austin, TX). Luminex color-coded tiny beads, called microspheres, into four distinct sets. Each bead set was coated with either IL-6, IL-1β, IL-10, or TNF-α antibodies, allowing the capture and detection of specific cytokines from a sample. Within the Luminex 100 analyzer, lasers excite the internal dyes that identify each microsphere particle, and any reporter dye captured during the assay. Many readings are made on each bead set, further validating the results.

In this way, xMAP technology allows multiplexing of all four cytokines within a single sample (Luminex corp).

Plasma samples were prepared using a mouse cytokine/chemokine Lincoplex kit (Linco Research, St. Charles, MO). A 96-well filter plate was prepared by blocking the wells with 200 µL assay buffer. Prepared standards, controls and 25µL of plasma were pipetted into prepared wells. 25µL of an antibody bead mixture containing beads specific for IL-6, IL-1β, IL-10 and TNF-α were pipetted into each well and placed on a plate shaker in the cold room overnight to optimize antibody binding. The plate was washed with 200 µL/well wash buffer and 25 µL detection antibody and 25 µL streptavidin-phycoerythrin was added to each well. The plate was placed on a plate shaker at room temperature for 30 min and the contents were vacuumed off. The plate was washed three times with 200 µL/well wash buffer and 100 µL/well sheath fluid was added to each well. The plate was counted on the Luminex 100 analyzer. All samples were fit to a logistical 5-spline curve specific for each cytokine.

Plasma Radioactivity

Plasma samples were deproteinized with 100 µL of barium hydroxide [$Ba(OH)_2$, 0.3 N] and 100 µL zinc sulfate [$ZnSO_4$, 0.3 N] as described by Somogyi (76). Samples were centrifuged (Hercules Biofuge Fresco, Kendro Laboratory Products, Germany) for 5 min at 13,000 rpm. Two samples were prepared for each time point. First, 100 µL was pipetted directly into glass scintillation vials along with 900 µL double distilled water and 10 mL of Ecolite+ scintillation fluid (ICN Biomedicals, Costa Mesa, CA). For the second sample, 100 µL were pipetted into glass scintillation vials and were evaporated at

50°C in a vacuum oven (Lab-line Instruments, Inc., Melrose Park, IL) to remove tritiated water. The dried residue was dissolved in 1 mL of double distilled water and 10 mL of Ecolite+. The [^{3}H] and [^{14}C] radioactivity was determined by double label liquid scintillation counting (Beckman LS 3801; Beckman Instruments, Inc., Irvine, CA) for 10 min. Quenching occurs when quenching agents in the sample cause a left shift of the energy spectrum. Thus, the scintillation counter was programmed to correct for the error caused by quenching. Quenching curves were created such that counts per minute (cpm) were converted to disintegrations per minute (dpm) by subtracting background cpm and then dividing by the counting efficiency for each sample. Data was corrected for spillover.

Recovery standards were prepared in order to determine the recovery of radioactive glucose during the deproteinization step. The 3-[^{3}H]-glucose infusate was diluted 1:200 (v:v) with saturated benzoic acid. The radioactivity was assessed in three types of standards. First, 100 μL of the diluted infusate (chemical standard, CS) with 10 mL of Ecolite+ was counted in triplicate. Second, 100 μL of diluted infusate was evaporated (chemical standard evaporated, CSE) in triplicate to ensure that [^{3}H] H_2O was removed from the sample. The dried residue was dissolved in 1 mL of double distilled water and 10 mL of Ecolite+. Finally, 100 μL of diluted infusate was treated in the same manner as the plasma samples (chemical recovery standard, CRS) by following the same deproteinization steps as outlined above. Recovery of radioactivity was calculated as the ratio of CSE to CRS, and all samples were corrected using this ratio.

^{14}C radioactivity was calculated on arterial plasma samples during the last 25 min of all metabolic studies in order to quantify the disappearance of [2-^{14}C]DG from the

plasma. [2-^{14}C]DG standards were prepared in order to determine the recovery of radioactive 2-deoxy-glucose. In short, 4 μL of [2-^{14}C]DG infusate was diluted 1:50 (v:v) with saline (mixture A). 50 μL of mixture A was diluted 1:20 (v:v) with dd water (mixture B) and 100 μL of mixture B was added to a glass scintillation vial with 900 μL dd water and 10 mL Ecolite+ scintillation fluid and counted.

Tissue Radioactivity

^{14}C radioactivity was determined independently on all tissues excised during all metabolic studies. Tissues were kept frozen while being weighed and homogenized in 1.5 mL of 0.5% perchloric acid. Homogenates were centrifuged (Beckman GS-6R, Beckman Instruments Inc., Irvine, CA) for 20 min at 3500rpm and 1.25 mL were pipetted into a fresh tube and neutralized to ~7.5pH with KOH. One aliquot from each tissue was counted directly to determine the combined [2-^{14}C]DG and [2-^{14}C]DG-6-phosphate ([2-^{14}C]DGP) radioactivity. A second aliquot from each tissue was treated with $Ba(OH)_2$ and $ZnSO_4$ to remove [2-^{14}C]DGP and any tracer incorporated in to glycogen (55) and then counted to determine [2-^{14}C]DG radioactivity. The value for [2-^{14}C]DGP is determined by subtracting the dpm value for [2-^{14}C]DG + [2-^{14}C]DGP from the dpm value for [2-^{14}C]DG. The accumulation of [2-^{14}C]DGP was normalized to tissue weight for each experiment.

Calculations

Glucose Turnover

The definition of glucose turnover is the rate of old glucose that is replaced by new glucose. Radioactively tagged glucose is used as a means to measure glucose turnover. In order to validate glucose turnover, several things must be assumed. It is important that the selected model of glucose kinetics is valid, the radioactively labeled and unlabeled glucose molecules are metabolized in the same manner, the measurement of glucose specific activity (SA) is accurate, and the radioactive label is irreversibly lost in the metabolism of the molecule.

In all metabolic experiments, the glucose pool was initially primed with a bolus of tracer (3-[^{3}H]-glucose) followed by a constant infusion of tracer. The purpose of priming the pool is so that an equilibrium between the tracer and tracee (endogenous non-labeled glucose) is established thus allowing SA (dpm/mg) to be in a steady state. Glucose turnover or production (R_a, rate of appearance) was calculated as the ratio of the tracer infusion rate and its SA in accordance with the following non-steady state equation:

$$R_a = [I - M\,(\delta SA/\delta t)]/SA \qquad (1)$$

where I is the tracer infusion rate (dpm/min), M is the mass of the pool of glucose (mg) and t is time (min).

Whole-body glucose utilization (R_d, rate of disappearance) was calculated using the following equation:

$$R_d = R_a - (V_d)\,(\delta A/\delta t) \qquad (2)$$

whereas V_d is the volume of distribution (mL/kg) of glucose. A value of 130 mL/kg is used in these calculations. A is the whole body glucose concentration and $\delta A/\delta t$ is its

derivative (50). Under no circumstance can $\delta A/\delta t$ be assumed to be zero in the non-steady state. Tracer-determined R_a and R_d were calculated according to the method of Wall *et al.* (92) as simplified by De Bodo *et al.* (23).

Glucose Clearance

Glucose clearance is used to assess the ability of peripheral tissues to remove glucose from the plasma in a manner that is independent of glucose concentration. Glucose clearance was calculated as follows:

$$\text{clearance} = R_d / [\text{glucose}]_{\text{arterial}} \quad (3)$$

where $[\text{glucose}]_{\text{arterial}}$ is the average blood glucose (mM) during the experimental period.

Tissue Glucose Uptake

Tissue glucose uptake is an index of how well the periphery clears glucose from the plasma under a certain metabolic state. Both concentration independent (R_i) and concentration dependent (R_g) indices of tissue glucose uptake were calculated according to the method of Kraegen *et al.* (42). R_i and R_g were calculated as follows:

$$R_i = [2\text{-}^{14}\text{C}]\text{DGP}_{\text{tissue}}/\text{AUC}\ [2\text{-}^{14}\text{C}]\text{DG}_{\text{plasma}} \quad (4)$$

$$R_g = (R_i)\ ([\text{glucose}]_{\text{plasma}}) \quad (5)$$

whereas $[2\text{-}^{14}\text{C}]\text{DGP}_{\text{tissue}}$ is the $[2\text{-}^{14}\text{C}]$DGP radioactivity (dpm/g) in the tissue, AUC $[2\text{-}^{14}\text{C}]\text{DG}_{\text{plasma}}$ is the area under the plasma $[2\text{-}^{14}\text{C}]$DG disappearance curve (dpm/mL/min), and $[\text{glucose}]_{\text{plasma}}$ is the average blood glucose (mM) during the experimental period.

All counts were normalized by standard infusate radioactivity before calculating R_i and R_g.

Statistical Analysis

Power calculations were conducted and it was determined that at least 8 animals were required per group to obtain sufficient statistical power to detect differences among the groups. All data are presented as mean ± SEM. Differences between groups were determined by ANOVA or repeated measures ANOVA when appropriate. The significance level was set at 0.05 (Sigma Stat, Port Richmond, CA).

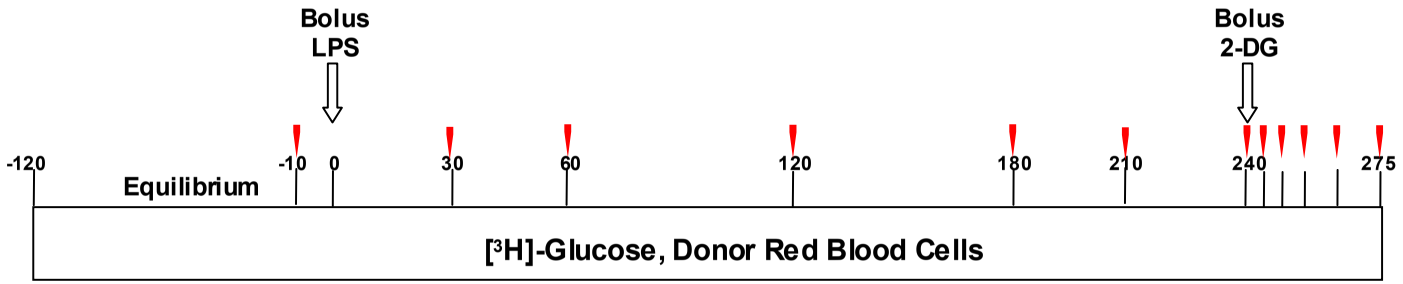

Fig. 1. **LPS Challenge.** IL-6$^{-/-}$ (n=13), IL-6 $^{+/-}$ (n=9) or IL-6$^{+/+}$ (n=10) mice undergo an LPS Challenge. ▼ Blood Sample.

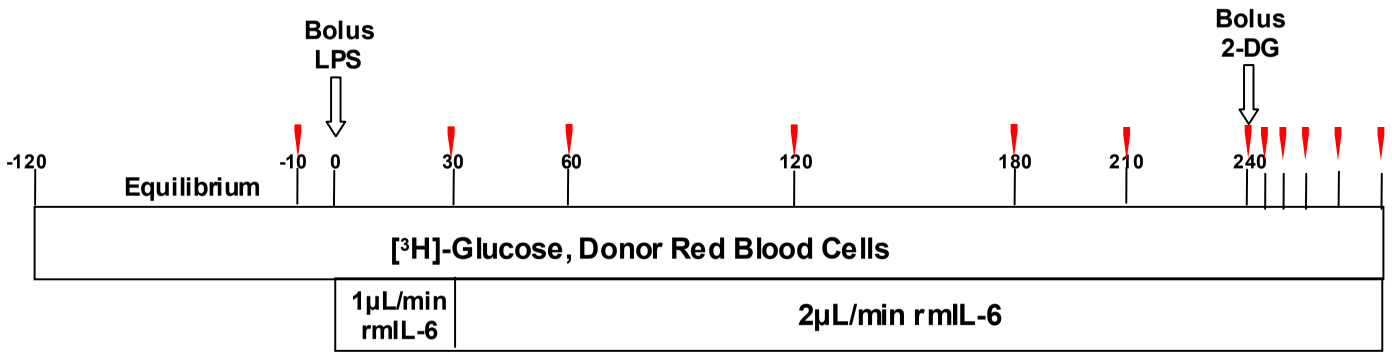

Fig. 2. **Biased Supplement of IL-6 During an LPS Challenge.** IL-6$^{-/-}$ (n=10) mice undergo a LPS Challenge with a constant infusion (1µL/min) of rmIL-6 starting at t=0. rmIL-6 infusion rate is increased (2µL/min) at t=30 for the remainder of the study. ▼ Blood Sample.

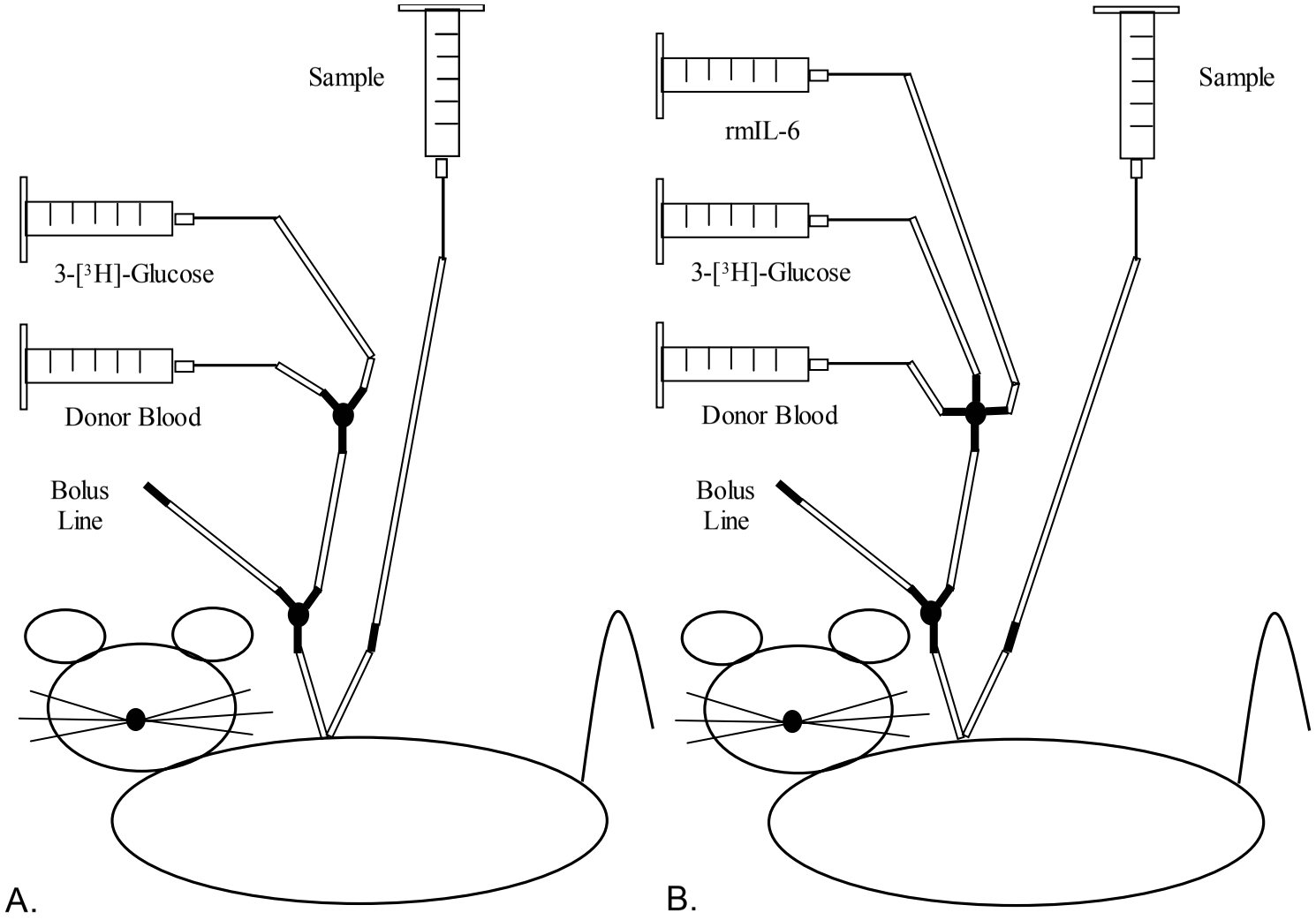

Figure 3: Experimental setup for A) LPS and B) LPS with IL-6 replacement studies.

CHAPTER III

THE IMPACT OF INTERLEUKIN-6 ON THE METABOLIC RESPONSE TO ENDOTOXIN *in vivo*

Specific Aims

The goal of this study was to examine the impact of Interleukin-6 (IL-6) on the metabolic response to endotoxin *in vivo*. The specific goals of this study were: 1) To characterize the metabolic response to endotoxin in the presence or absence of the IL-6 protein, and 2) To test whether the metabolic response to endotoxin observed in wild type mice can be recapitulated by infusing physiological levels of rmIL-6 into IL-6 knockout mice.

Hypothesis

The absence of IL-6 attenuates the hypoglycemic response to acute endotoxemia.

Results

Glucose Metabolism: The arterial blood glucose concentrations were similar during the basal period in the IL-6 $^{+/-}$ (HET), IL-6 $^{-/-}$ (KO), and IL-6 $^{-/-}$ with rmIL-6 replacement (KO + IL-6) groups (144±14, 145±9, 158±6 mg/dl; respectively), but IL-6$^{+/+}$ (WT) mice had a significantly lower basal arterial blood glucose concentration (102±11 mg/dl; $P<0.005$) (Figures 4 and 16). Following the bolus of endotoxin, arterial blood glucose concentrations increased in all groups, with the largest increase noticeable at 60 min. Arterial blood glucose fell below baseline for all groups by 240 min, with the WT group reaching glucose concentrations deemed hypoglycemic (70±8 mg/dl; WT).

R_a (Figures 5 and 17), R_d (Figures 6 and 18), and glucose clearance (Figures 7 and 19) were calculated using a non-steady state equation. Basal conditions can be considered steady state since the animal was not experiencing any sudden changes in R_a, R_d, clearance, or metabolism. Therefore, all groups had similar basal values for R_d as observed for R_a since $R_d = R_a$ in steady state conditions. During basal conditions, glucose clearance was similar in all groups.

KO displayed similar glucose clearance patterns as KO + IL-6 within the first 30 min (Figure 7). During this time, the rate of glucose clearance decreased in both of these groups. R_a remained comparatively unchanged over basal values in both groups.

The most profound changes in arterial glucose occurred between 30 and 180 min following the LPS bolus. During this time, R_a and R_d were matched in all groups. There was little change in R_a, R_d, and clearance in WT and HET, while KO experienced a significant change in both R_a and R_d ($P<0.010$) that was accompanied by an increase in glucose clearance ($P<0.037$) over the 30 min time period.

During the 180 to 210 min time period, arterial glucose was below baseline in all groups and glucose clearance was increased in all groups with the greatest increase occurring in HET and KO + IL-6 ($P<0.003$).

By the end of the study, R_a and R_d were equivalent in all groups and were similar to values observed during the basal period. Glucose clearance remained unchanged compared with values observed in the 180 to 210 time period.

Cytokine Concentration: Blood IL-6 levels rose simultaneously in WT and HET (386±138 to 14606±404 to 14880±653 and 21±6 to 14313±476 to 14050±543pg/ml; respectively; basal to 180 to 275 min), although HET experienced a delayed rise

compared to WT (Figure 20). As expected, IL-6 in KO was undetectable throughout the length of the study. The goal of the KO + IL-6 study was to recapitulate the levels of IL-6 observed in WT with the hypothesis that other cytokine, hormonal, and metabolic patterns would in turn mimic that of WT. The IL-6 profile in KO + IL-6 (12±6 to 14089±376 to 14402±283 pg/mL; basal to 180 to 275 min) was successfully matched to WT (Figure 8).

IL-1 was at the lower limits of detection in the basal period in all groups. IL-1 levels increased by 180 min and were similar in all groups. These levels continued to rise at the end of the study, with the largest difference being between HET and KO + IL-6 (436±97 and 262±63 pg/mL; respectively) (Figures 9 and 21).

TNF-α and IL-10 were low in the basal period in all groups. The increase observed at 180 min was equal among all groups in both TNF-α and IL-10. Interestingly, WT was the only group that experienced a rapid increase in TNF-α at 30 min (Figures 10 and 22) and KO was the only group that experienced a rapid increase in IL-10 by 30 min (Figures 11 and 23). Conversely, the rise in TNF-α in HET, KO, and KO + IL-6 did not reach ~1000 pg/mL by 30 min. IL-10 remained equally elevated in all groups at the end of the study. TNF-α remained equally elevated at the end of the study in WT, HET, and KO + IL-6 whereas KO was the only group that actually declined.

Hormone Concentration: The insulin concentration was nearly the same in all groups at the basal time point although KO had a higher basal insulin level ($P<0.032$) (Figure 12). Insulin levels in HET and WT were matched (0.22±0.05 and 0.21±0.03 ng/mL, respectively) (Figure 24) while KO had the most dramatic decrease over basal of any

group (0.41±0.07 ng/mL). KO + IL-6 displayed an intermediate insulin value at the end of the study (0.31±0.09 ng/mL) (Figure 12).

Glucagon was similar in all groups except for WT at the basal time point (157±29, 68±11, 53±10, and 72±16, and pg/mL; WT, HET, KO, and KO + IL-6 respectively) (Figures 13 and 25). By the end of the study, there was very little change in glucagon in WT, KO and KO + IL-6, with the greatest increase over basal being in HET.

Epinephrine was at the lower limits of the assay in all groups at the basal time point. All groups experienced a rise in epinephrine at 30 min. By the end of the study, epinephrine values were equal to values observed at 30 min in HET, KO, and KO + IL6 (114±47, 109±40, and 63±19 pg/mL; respectively) and significantly higher in WT (439±115 pg/mL; $P<0.001$) at 275 min (Figures 14 and 26).

Norepinephrine was also variable in all groups at the basal time point with WT and KO (124±26 and 137±19 pg/mL; respectively) values being significantly different than HET and KO + IL-6 (259±74 and 226±26 pg/mL; respectively; $P<0.050$). At 30 min, all groups were the same and this remained the case until the end of the study (Figures 15 and 27).

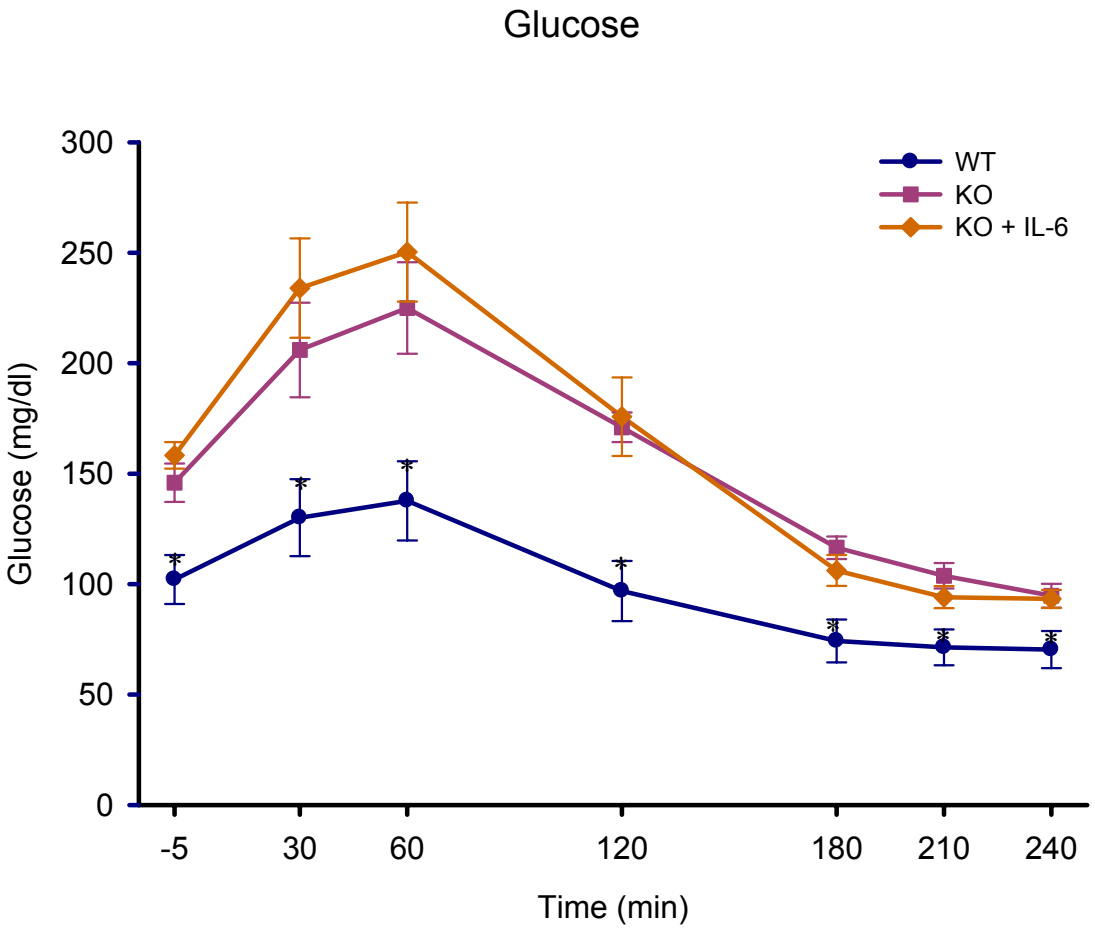

Figure 4: The plasma concentration of glucose in mg/dL in WT, KO, and KO + IL-6. Data are expressed as mean ± SE. * P<0.050

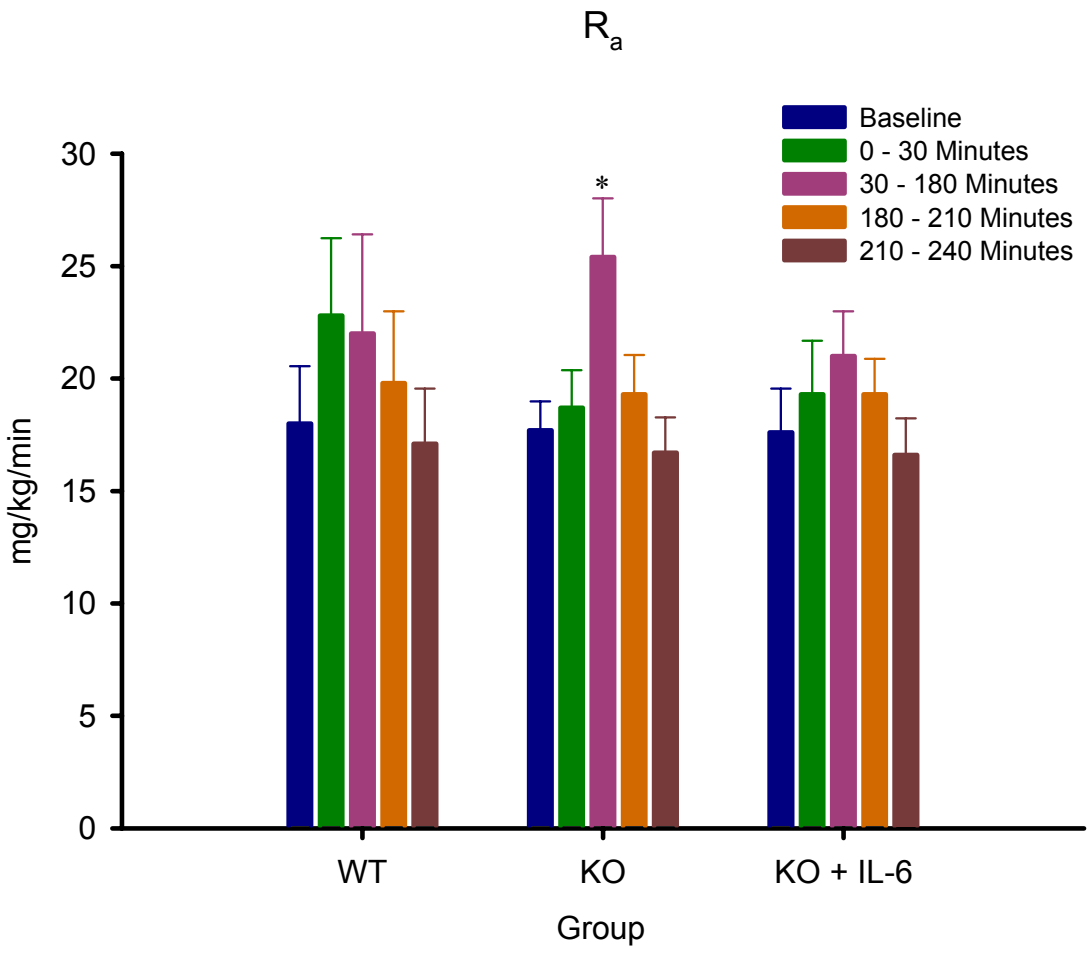

Figure 5: The rate of glucose production (R_a) in mg/kg/min in WT, KO, and KO + IL-6. Data are expressed as mean ± SE. * P<0.050

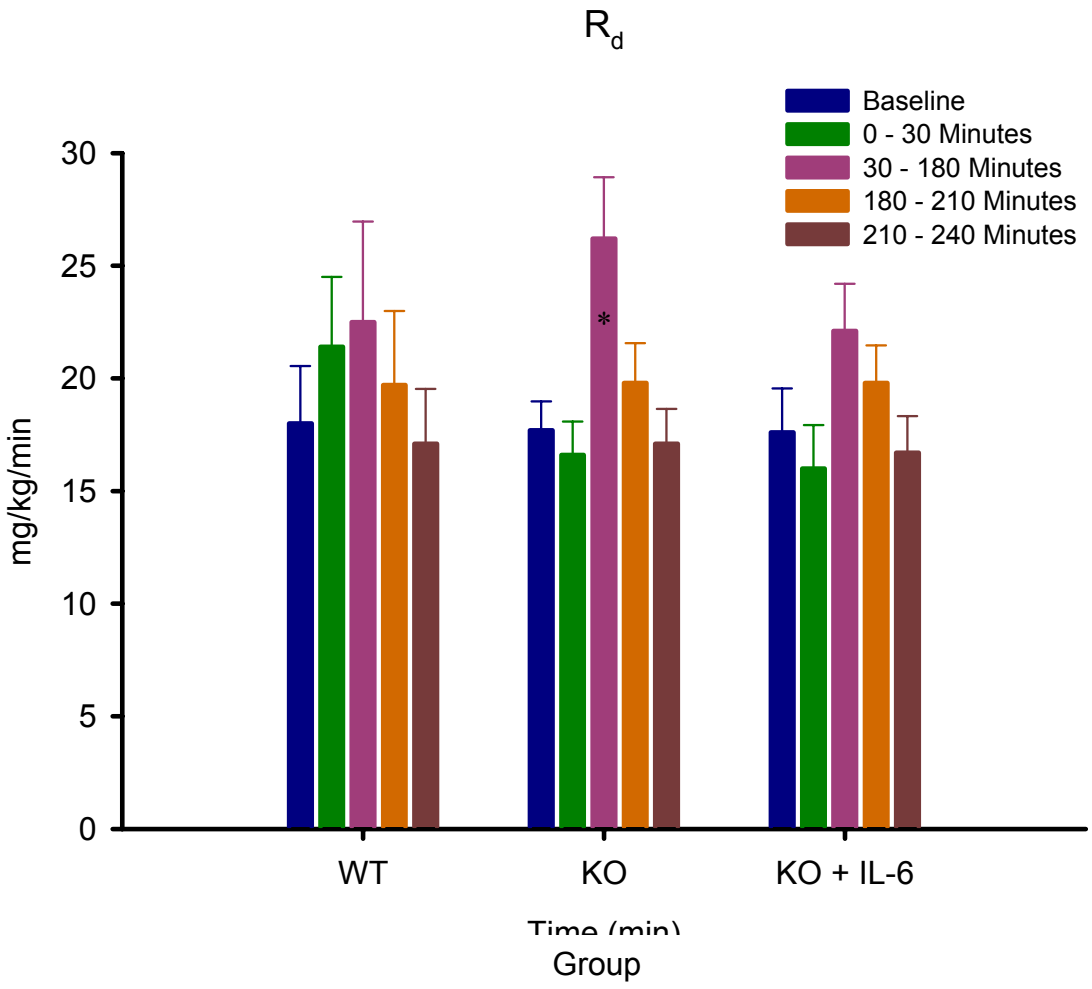

Figure 6: The rate of glucose utilization (R_d) in mg/kg/min in WT, KO, and KO + IL-6. Data are expressed as mean ± SE. * P<0.050

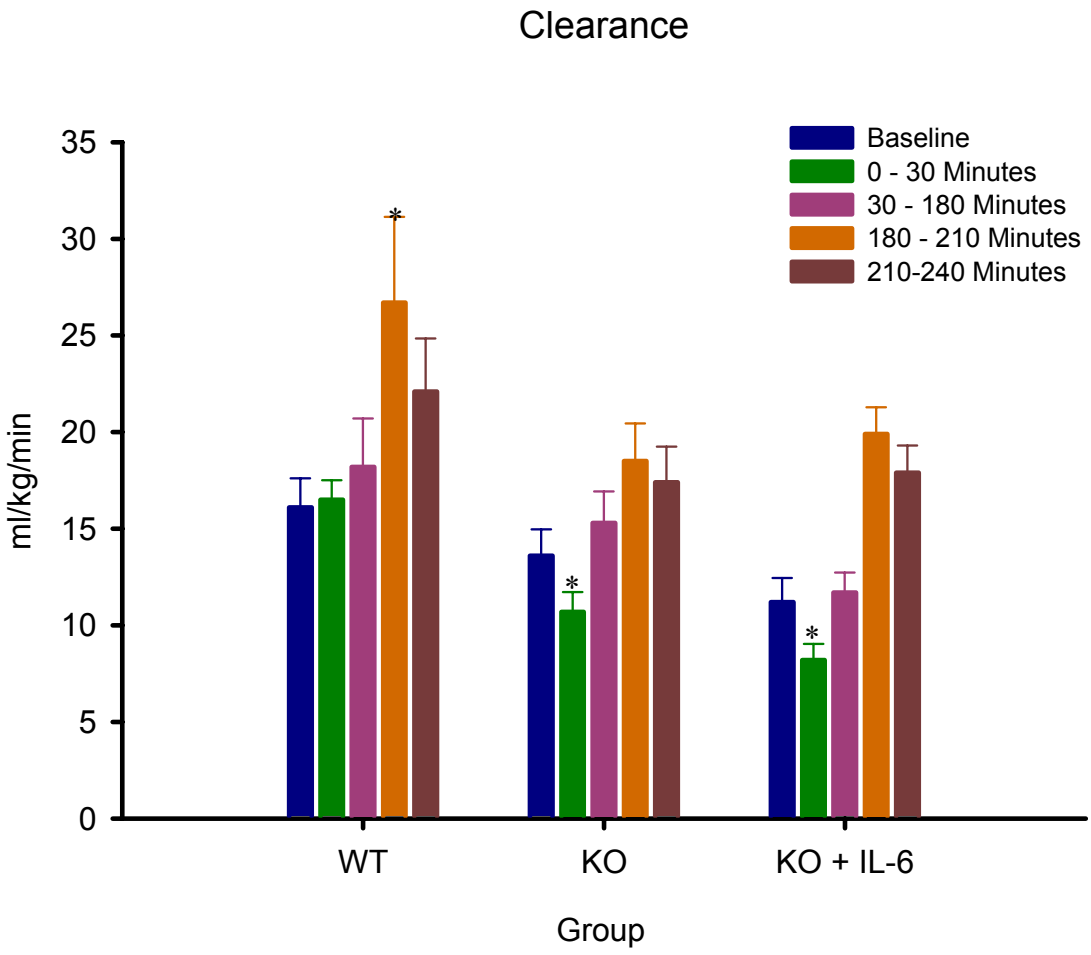

Figure 7: The rate of glucose clearance in ml/kg/min in WT, KO, and KO + IL-6. Data are expressed as mean ± SE. * P<0.050

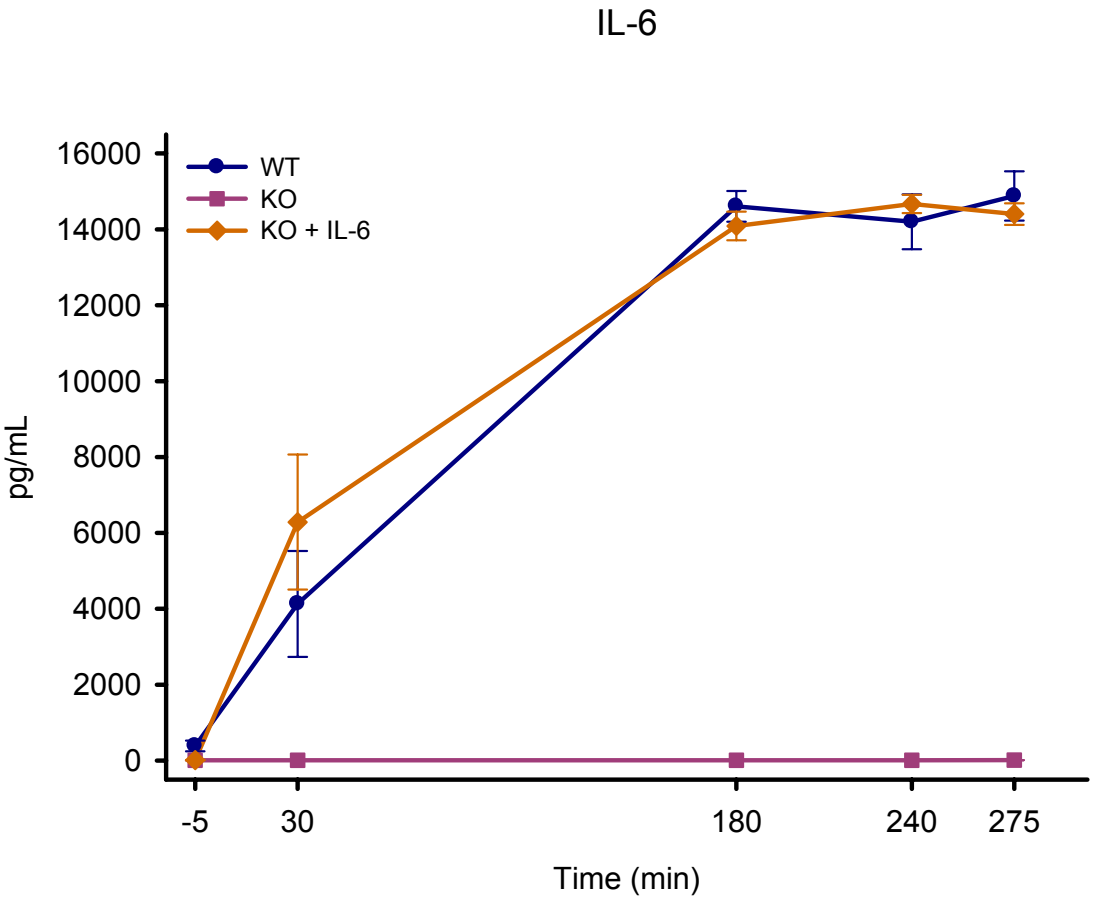

Figure 8: The plasma concentration of Interleukin-6 (IL-6) in pg/mL in WT, KO, and KO + IL-6. Data are expressed as mean ± SE.

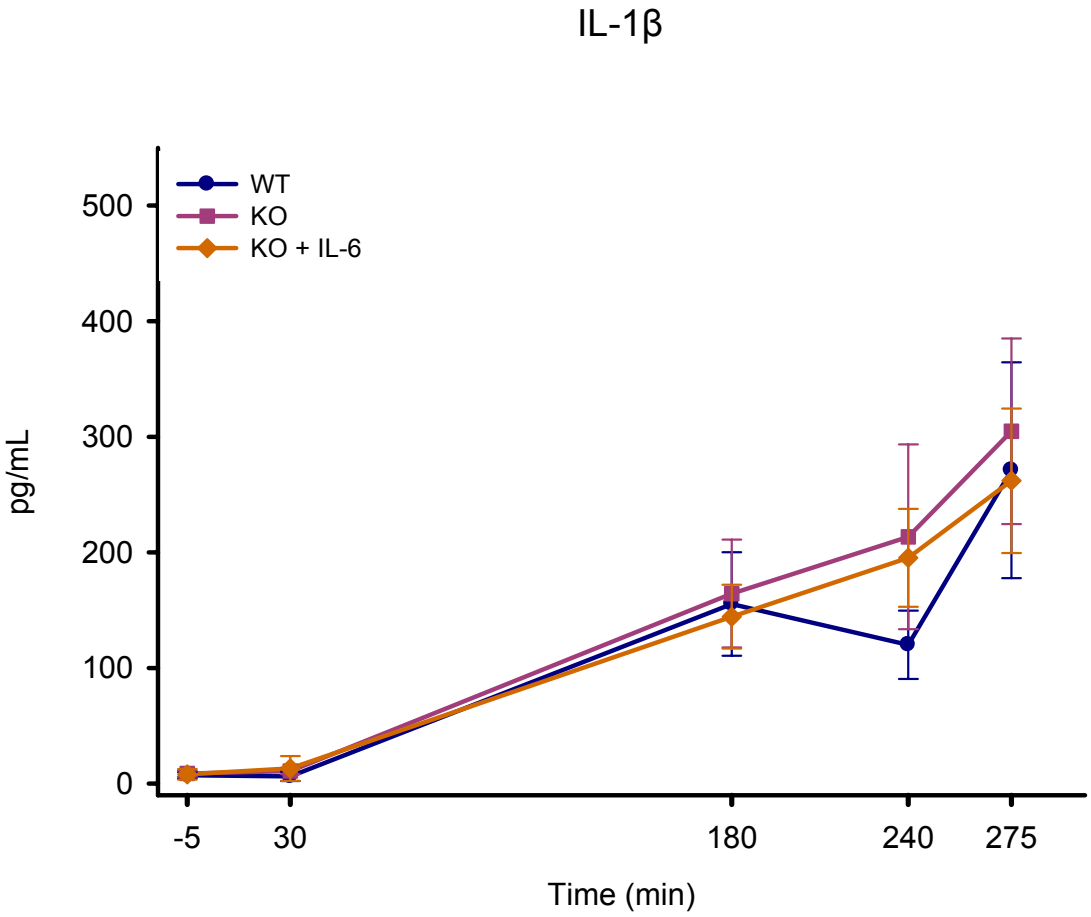

Figure 9: The plasma concentration of Interleukin-1β in pg/mL in WT, KO, and KO + IL-6. Data are expressed as mean ± SE.

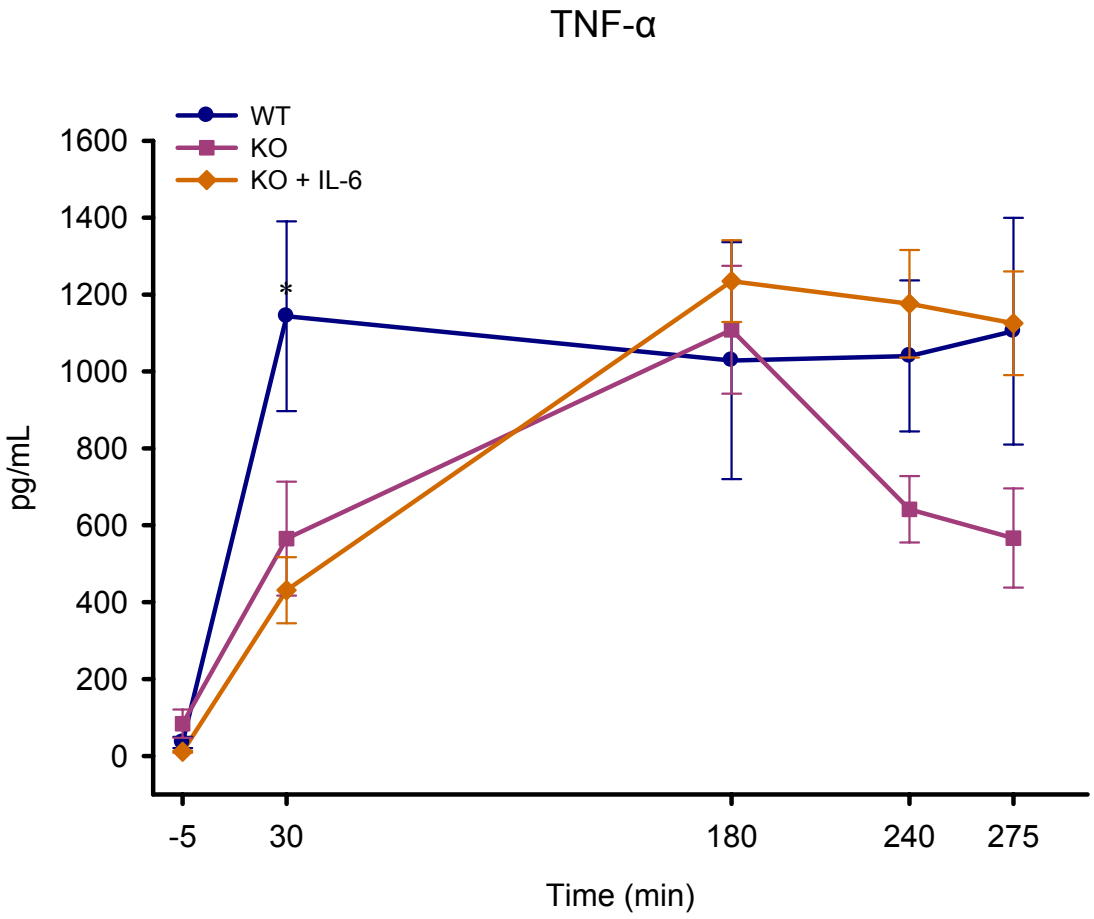

Figure 10: The plasma concentration of tumor necrosis factor-α (TNF-α) in pg/mL in WT, KO, and KO + IL-6. Data are expressed as mean ± SE. * P<0.050

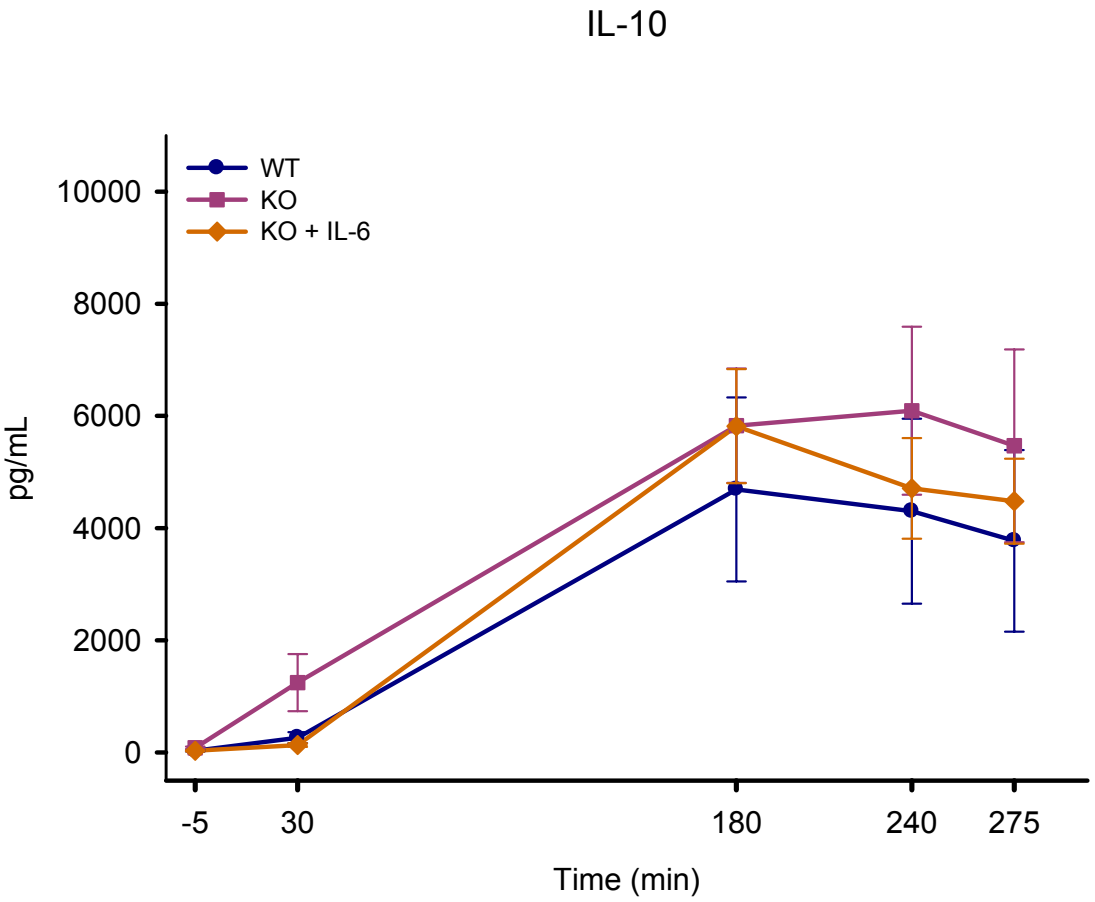

Figure 11: The plasma concentration of Interleukin-10 (IL-10) in pg/mL in WT, KO, and KO + IL-6. Data are expressed as mean ± SE.

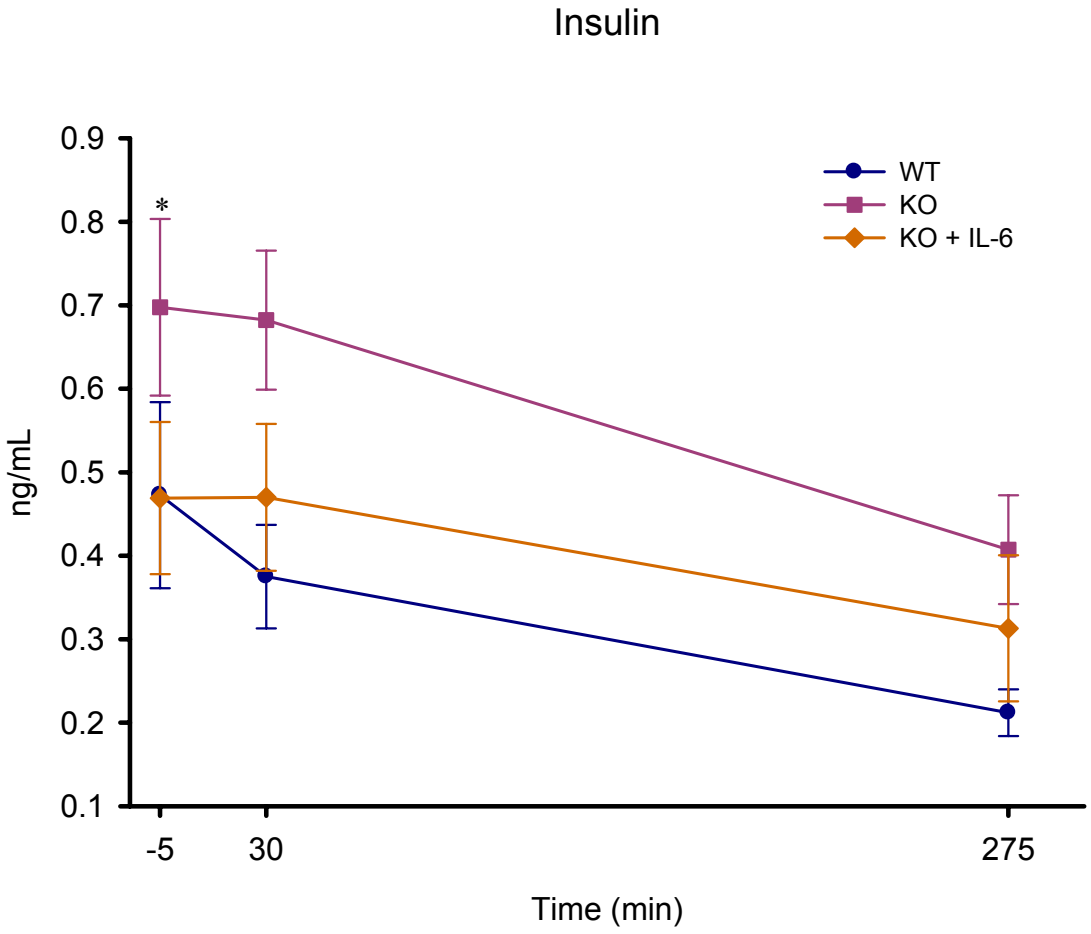

Figure 12: The plasma concentration of insulin in ng/mL in WT, KO, and KO + IL-6. Data are expressed as mean ± SE. * P<0.050

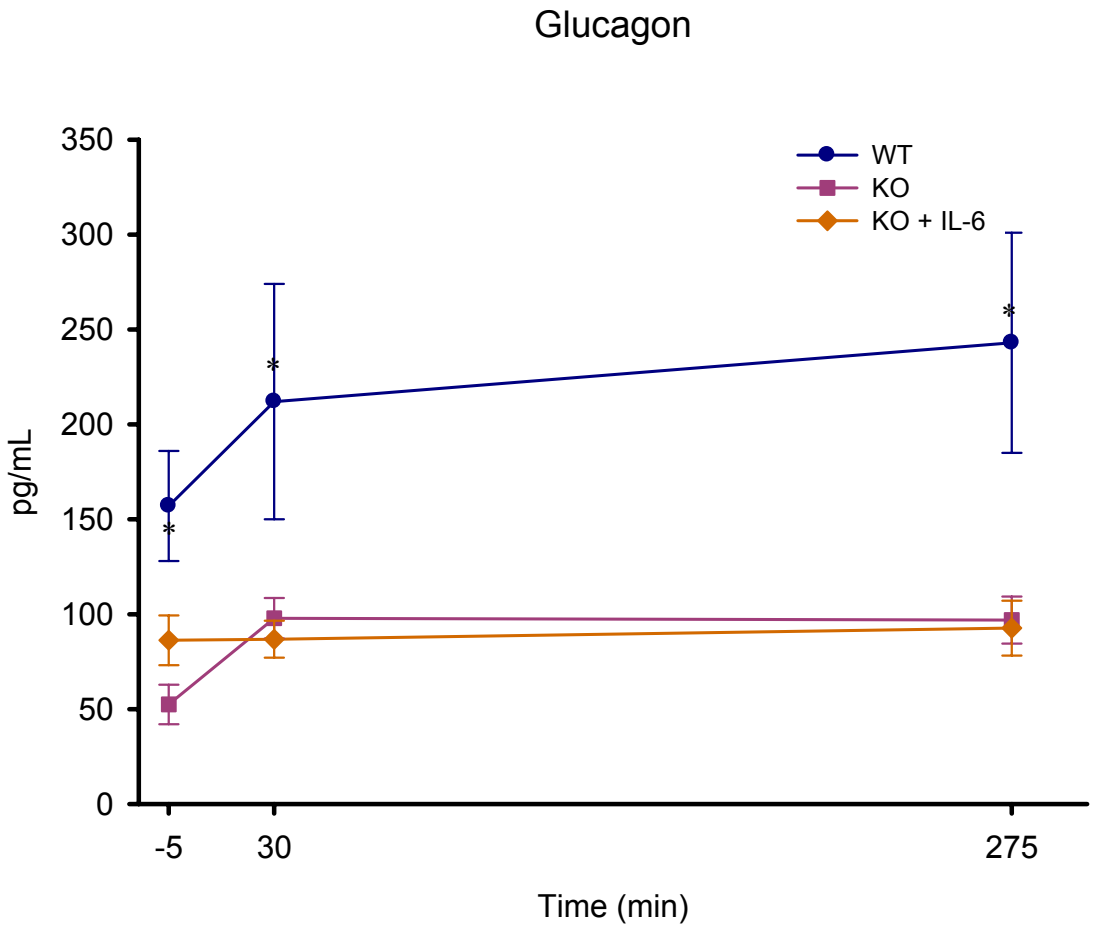

Figure 13: The plasma concentration of glucagon in pg/mL in WT, KO, and KO + IL-6. Data are expressed as mean ± SE. * P<0.050

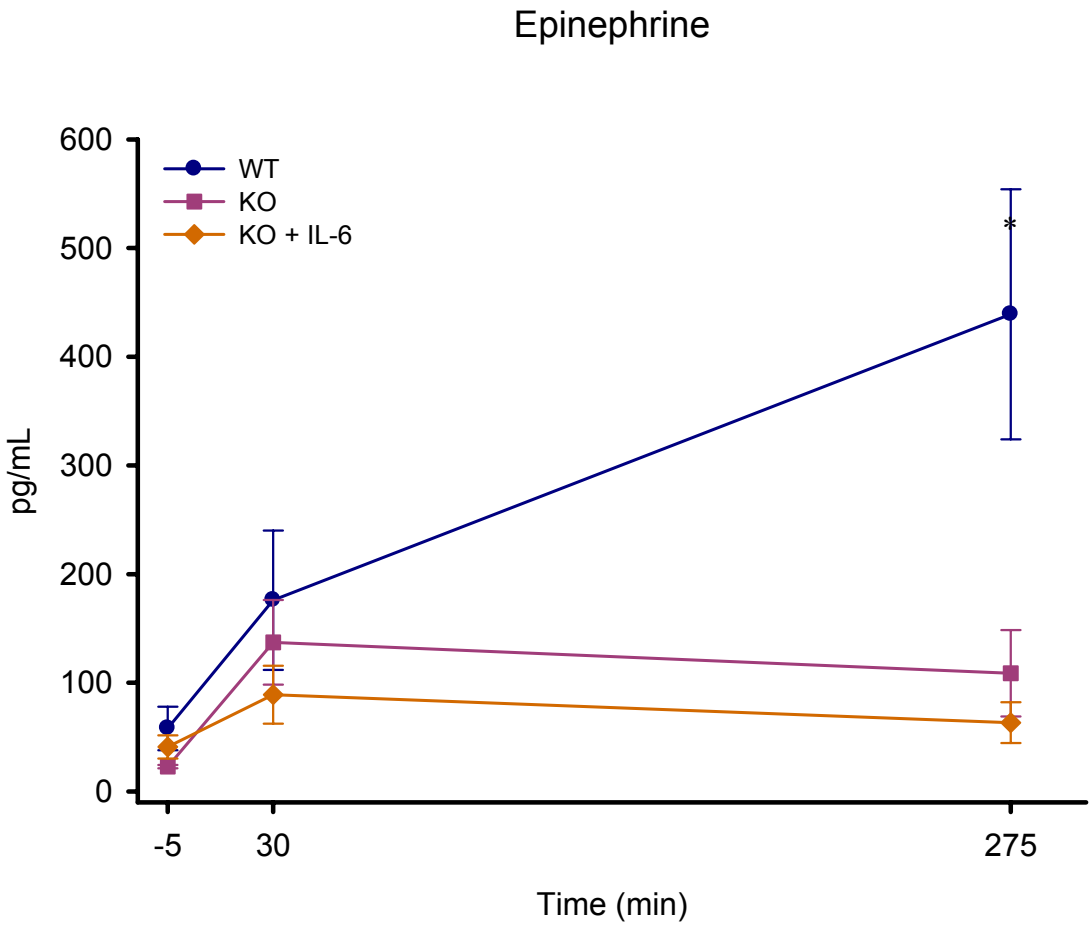

Figure 14: The plasma concentration of epinephrine in pg/mL in WT, KO, and KO + IL-6. Data are expressed as mean ± SE. * P<0.050

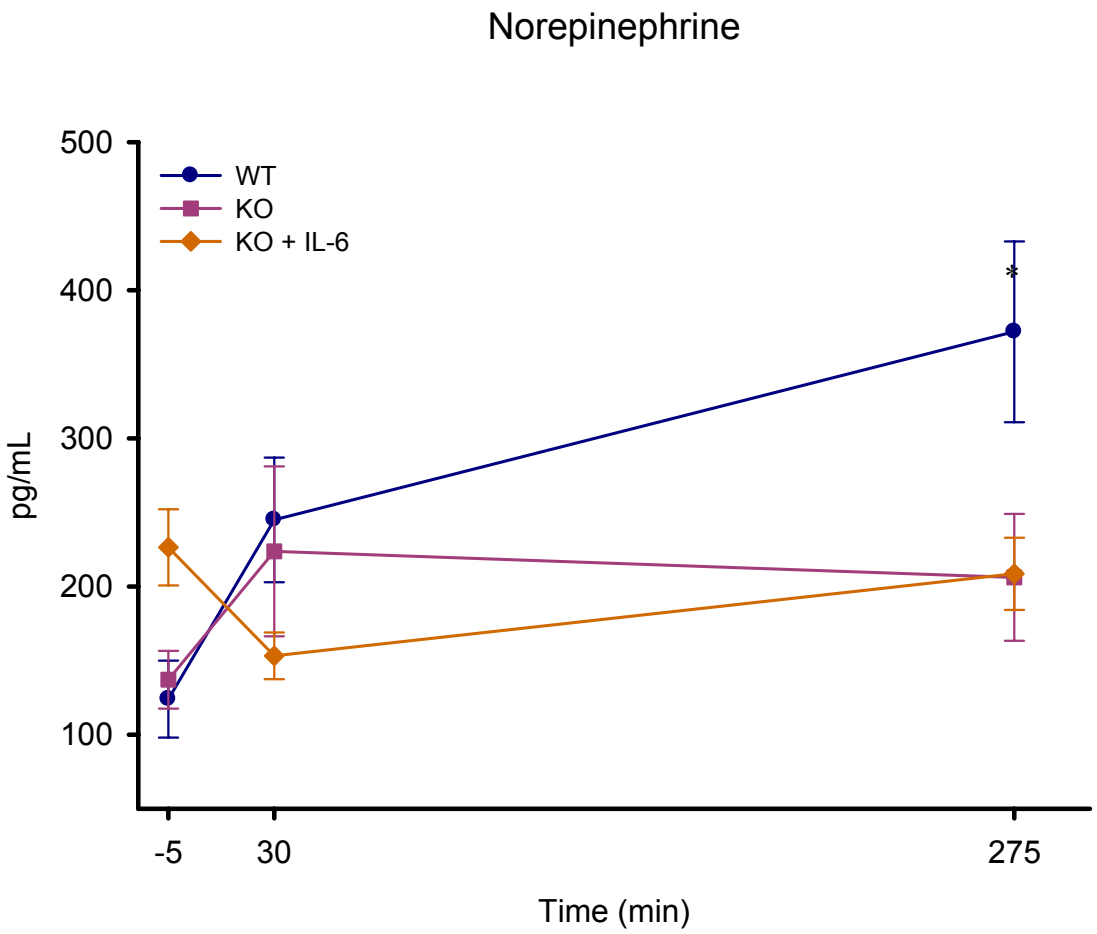

Figure 15: The plasma concentration of norepinephrine in pg/mL in WT, KO, and KO + IL-6. Data are expressed as mean ± SE. * P<0.050

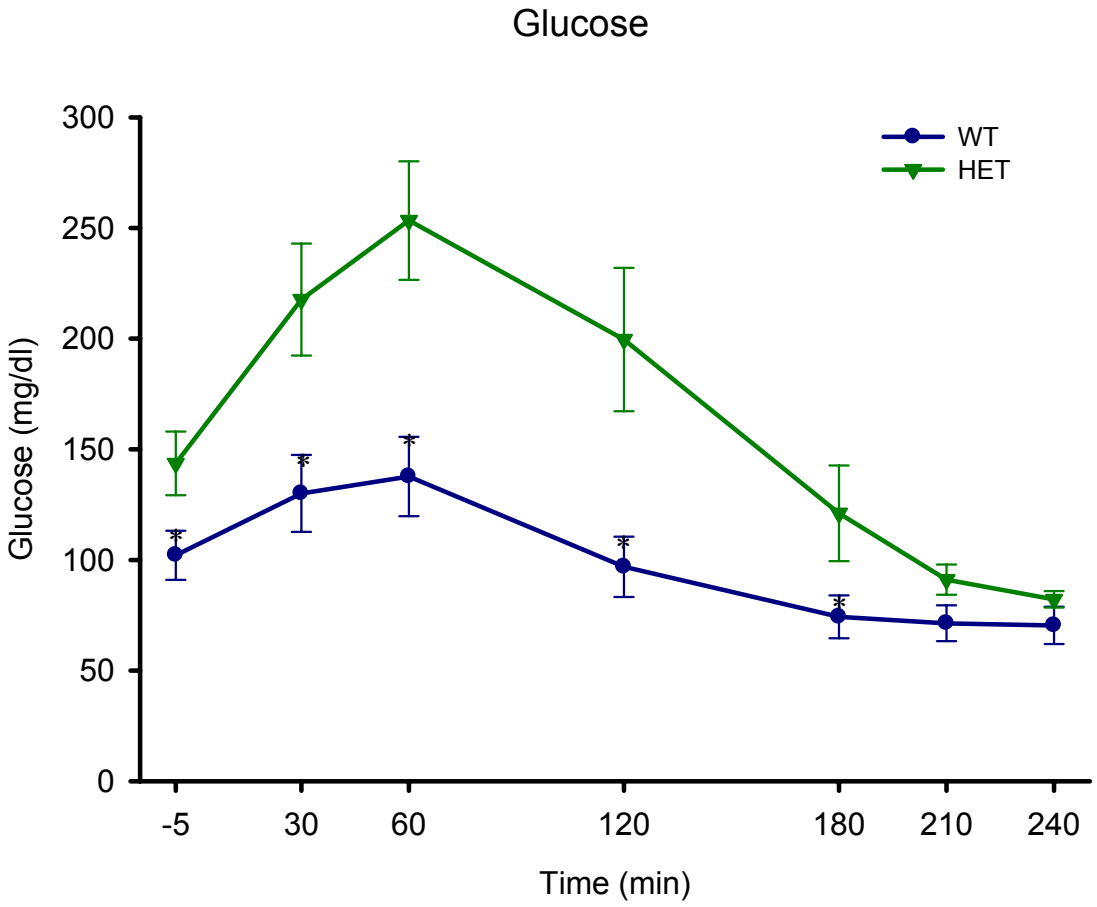

Figure 16: The plasma concentration of glucose in mg/dl in WT and HET. Data are expressed as mean ± SE. * P<0.050

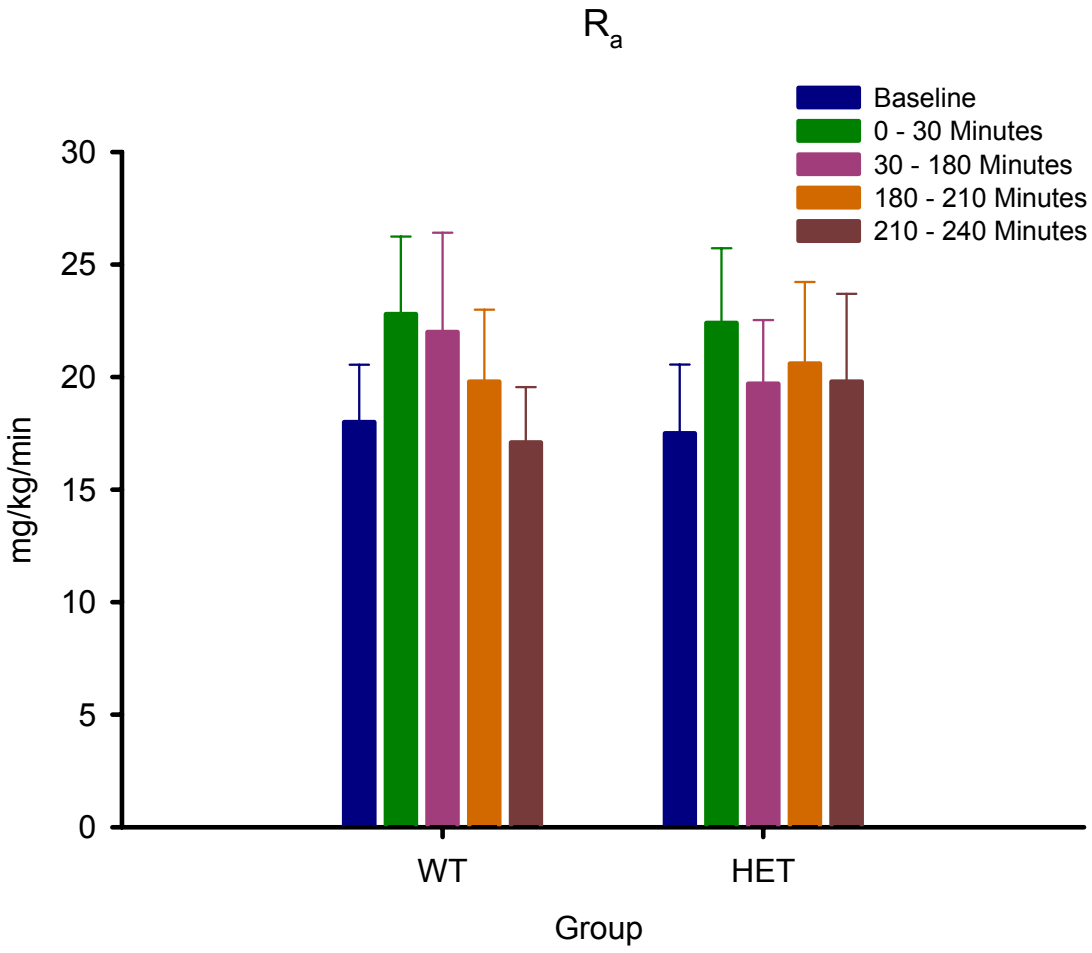

Figure 17: The rate of glucose production (R_a) in mg/kg/min in WT and HET. Data are expressed as mean ± SE.

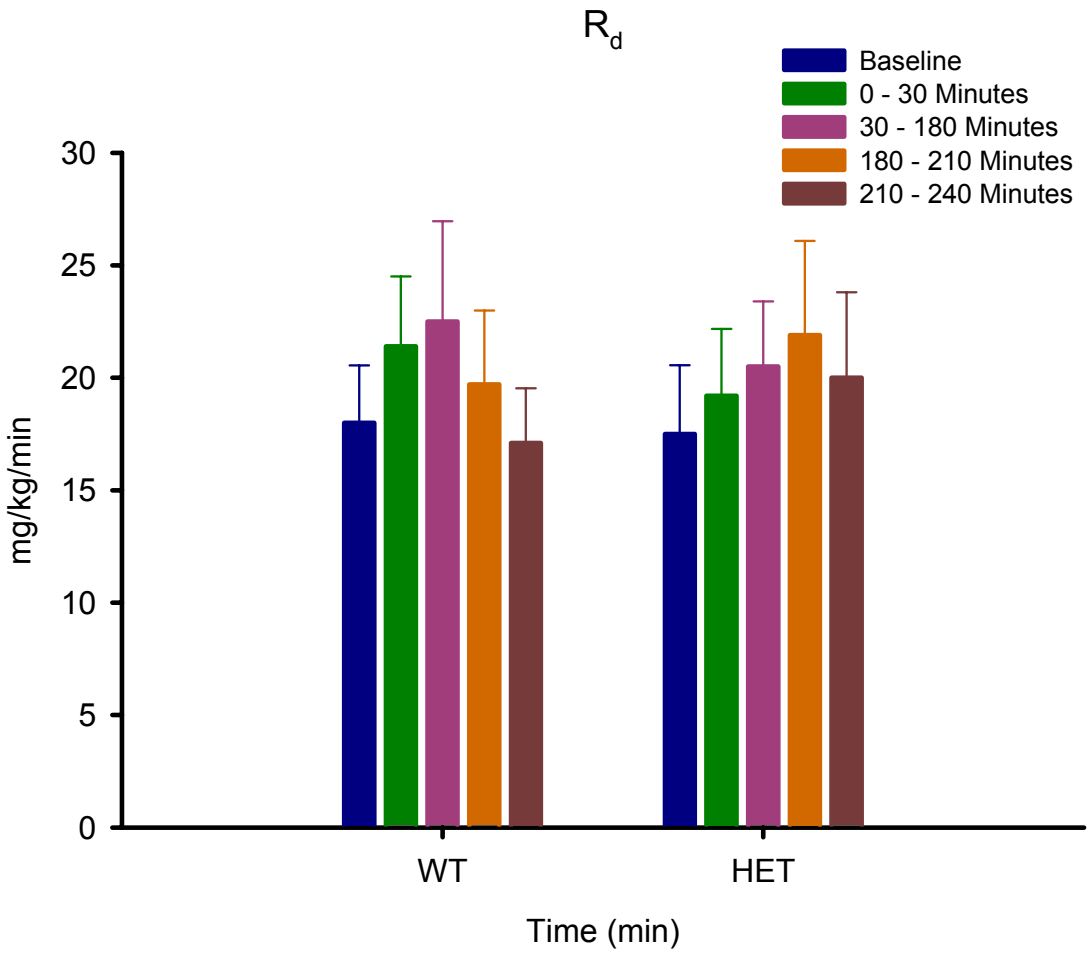

Figure 18: The rate of glucose utiliz Group mg/kg/min in WT and HET. Data are expressed as mean ± SE.

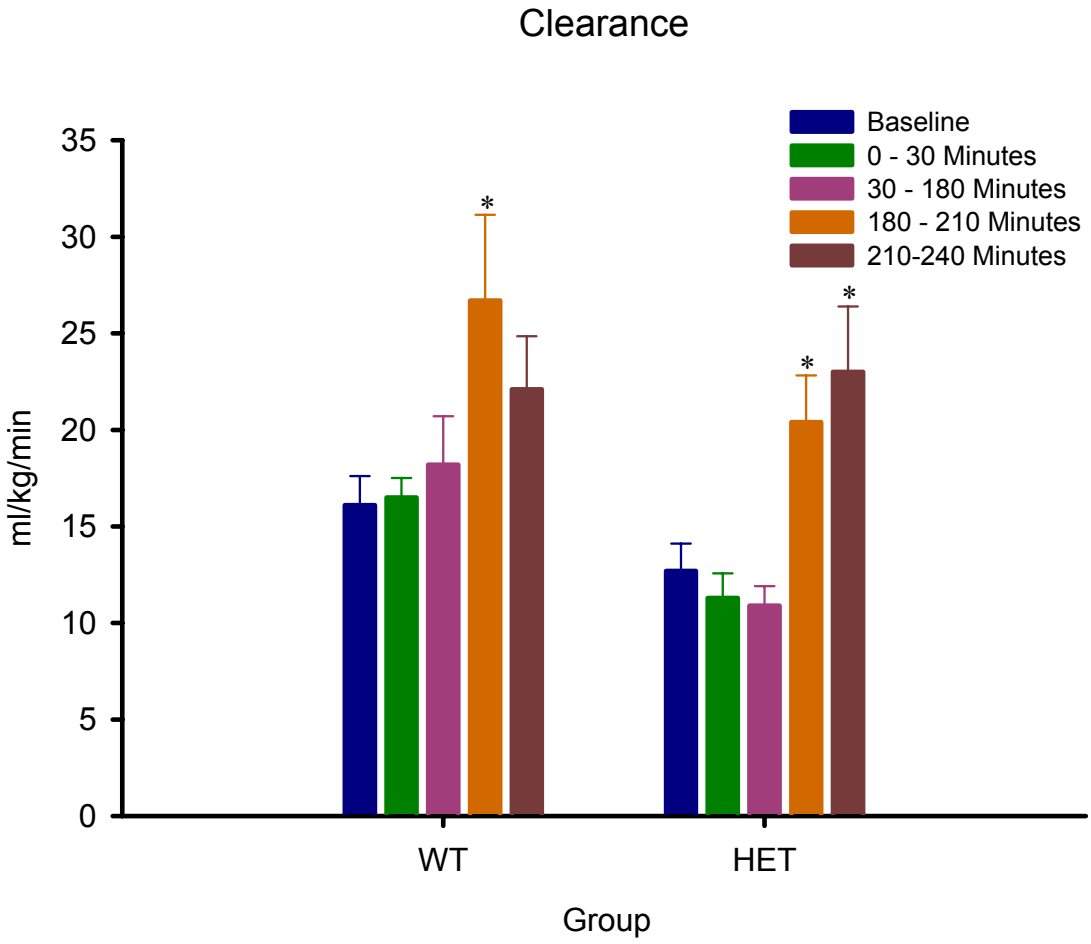

Figure 19: The rate of glucose clearance in ml/kg/min in WT and HET. Data are expressed as mean ± SE. * P<0.050

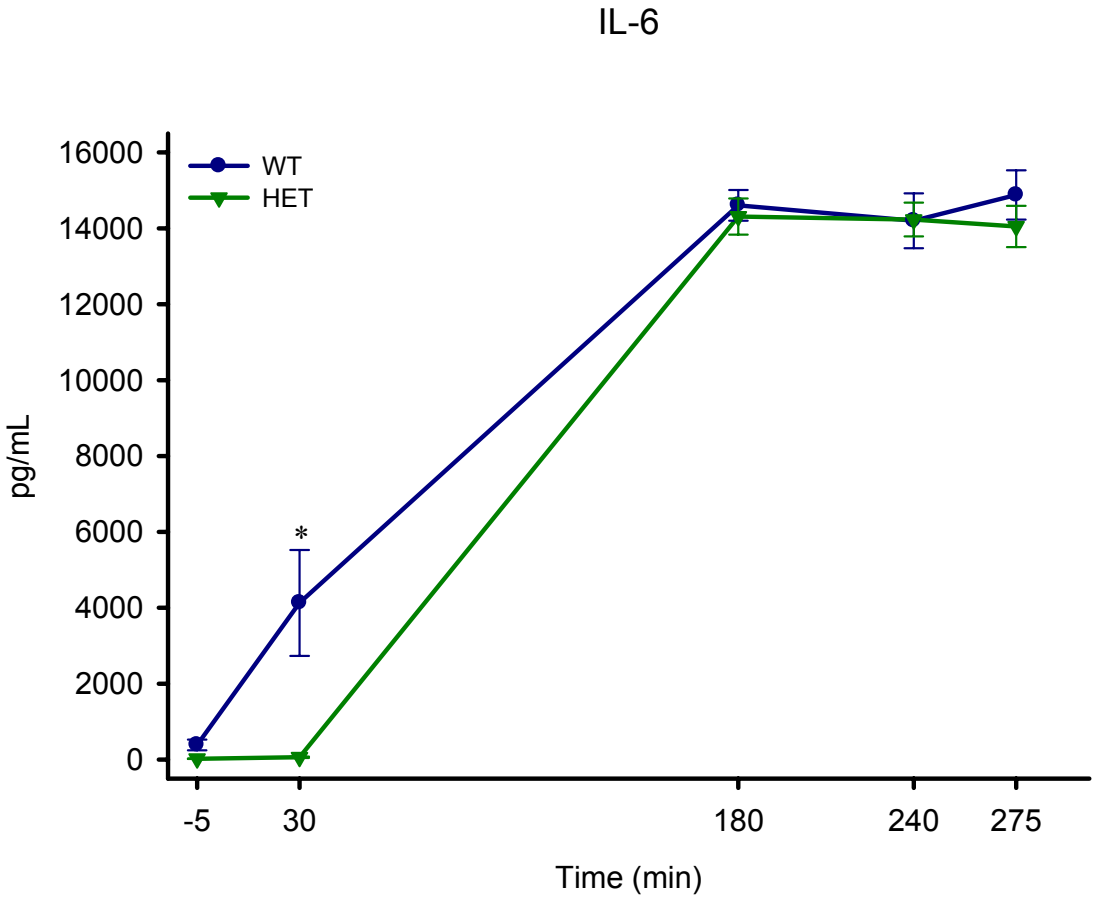

Figure 20: The plasma concentration of Interleukin-6 (IL-6) in pg/mL in WT and HET. Data are expressed as mean ± SE. * P<0.050

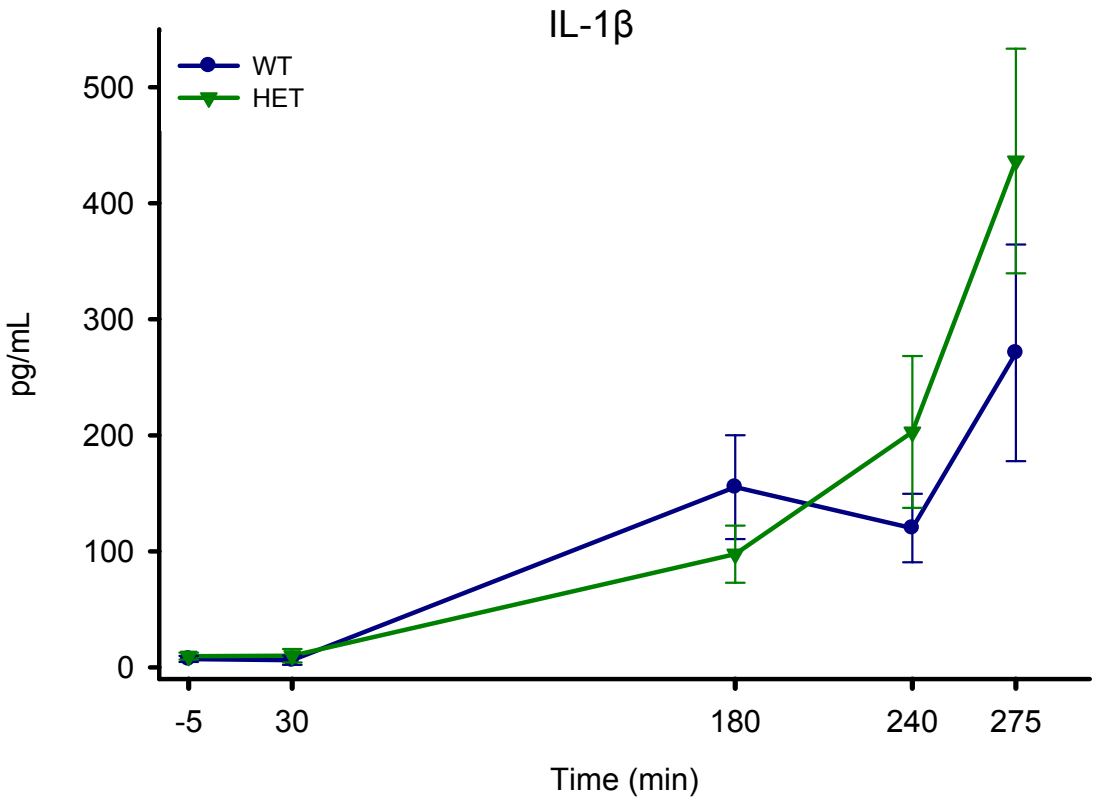

Figure 21: The plasma concentration of Interleukin-1β in pg/mL in WT and HET. Data are expressed as mean ± SE.

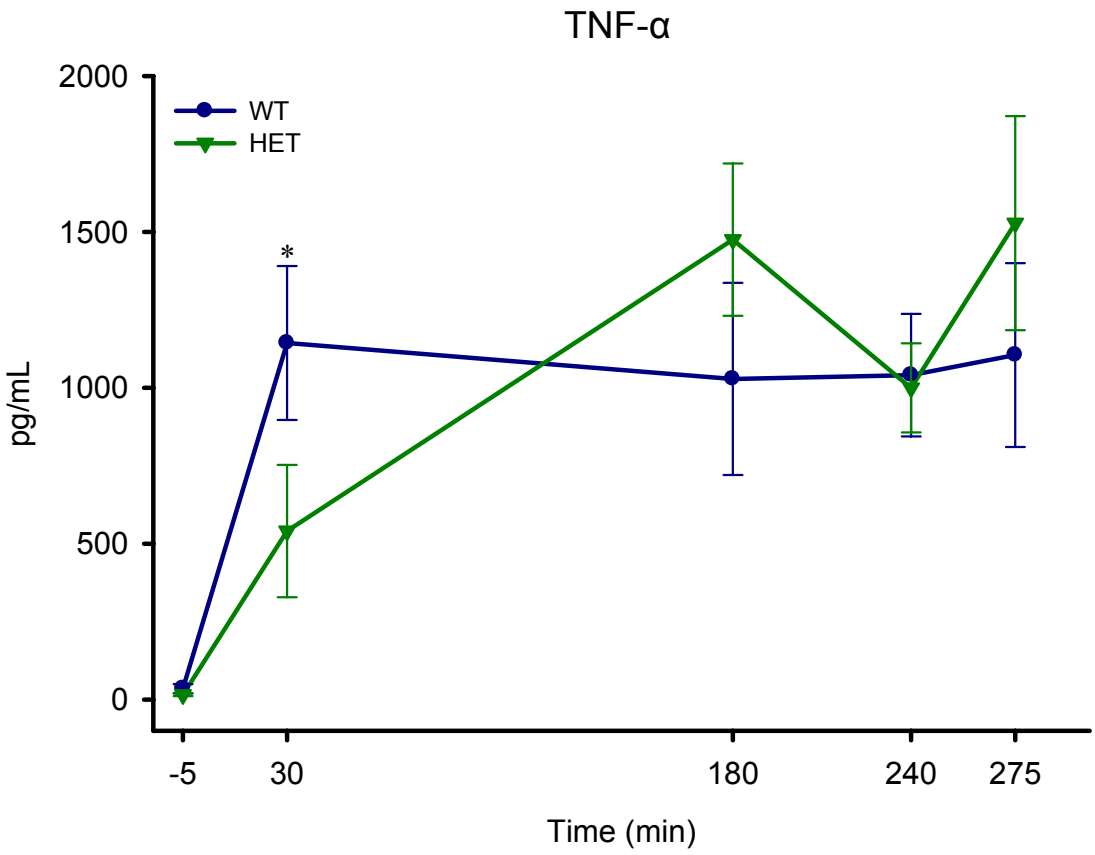

Figure 22: The plasma concentration of tumor necrosis factor-α (TNF-α) in pg/mL in WT and HET. Data are expressed as mean ± SE. * P<0.050

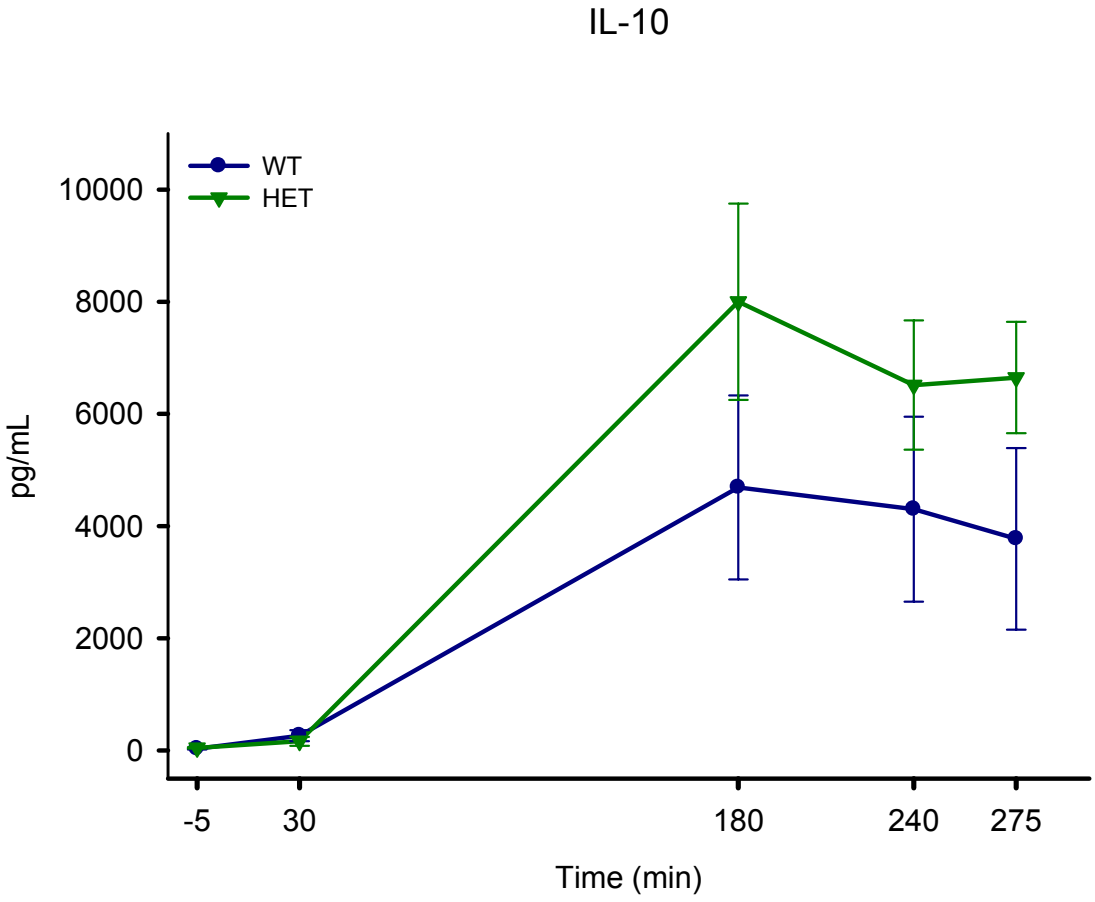

Figure 23: The plasma concentration of Interleukin-10 (IL-10) in pg/mL in WT and HET. Data are expressed as mean ± SE.

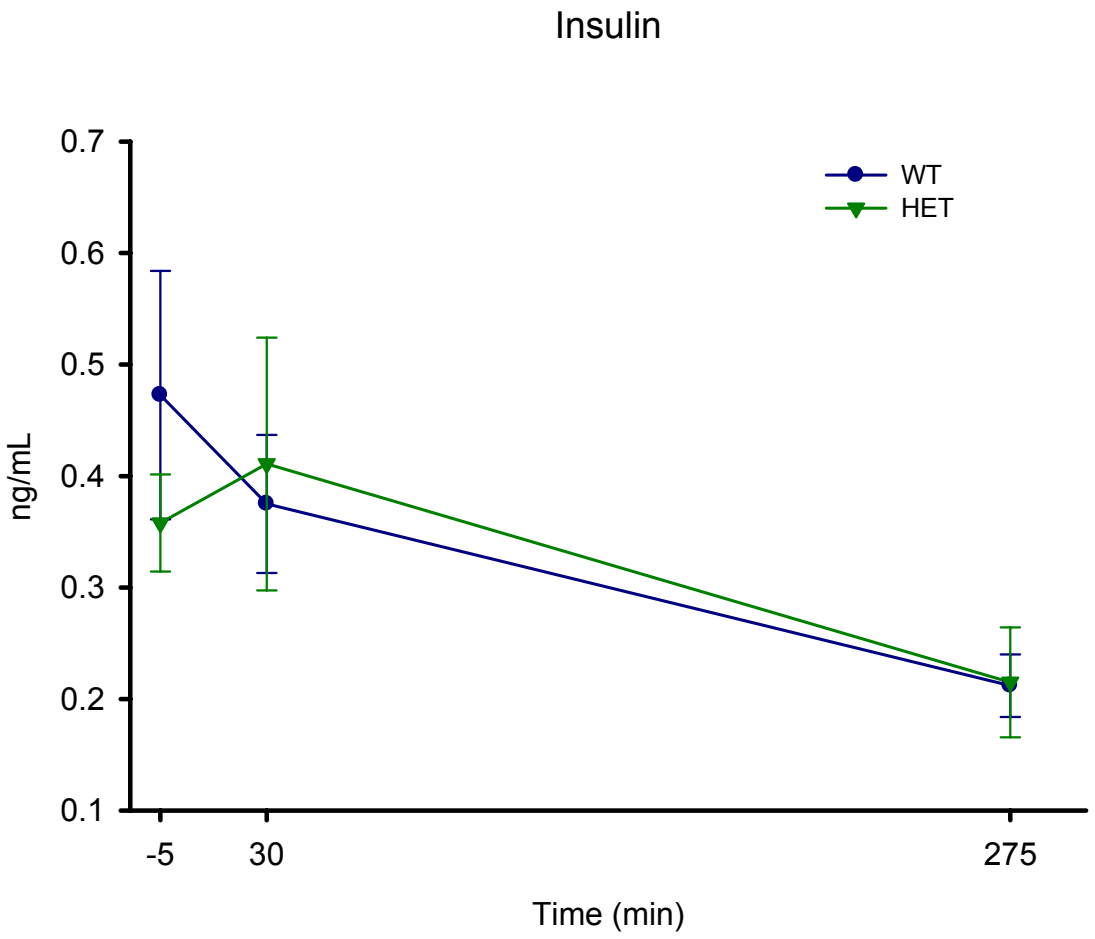

Figure 24: The plasma concentration of insulin in ng/mL in WT and HET. Data are expressed as mean ± SE.

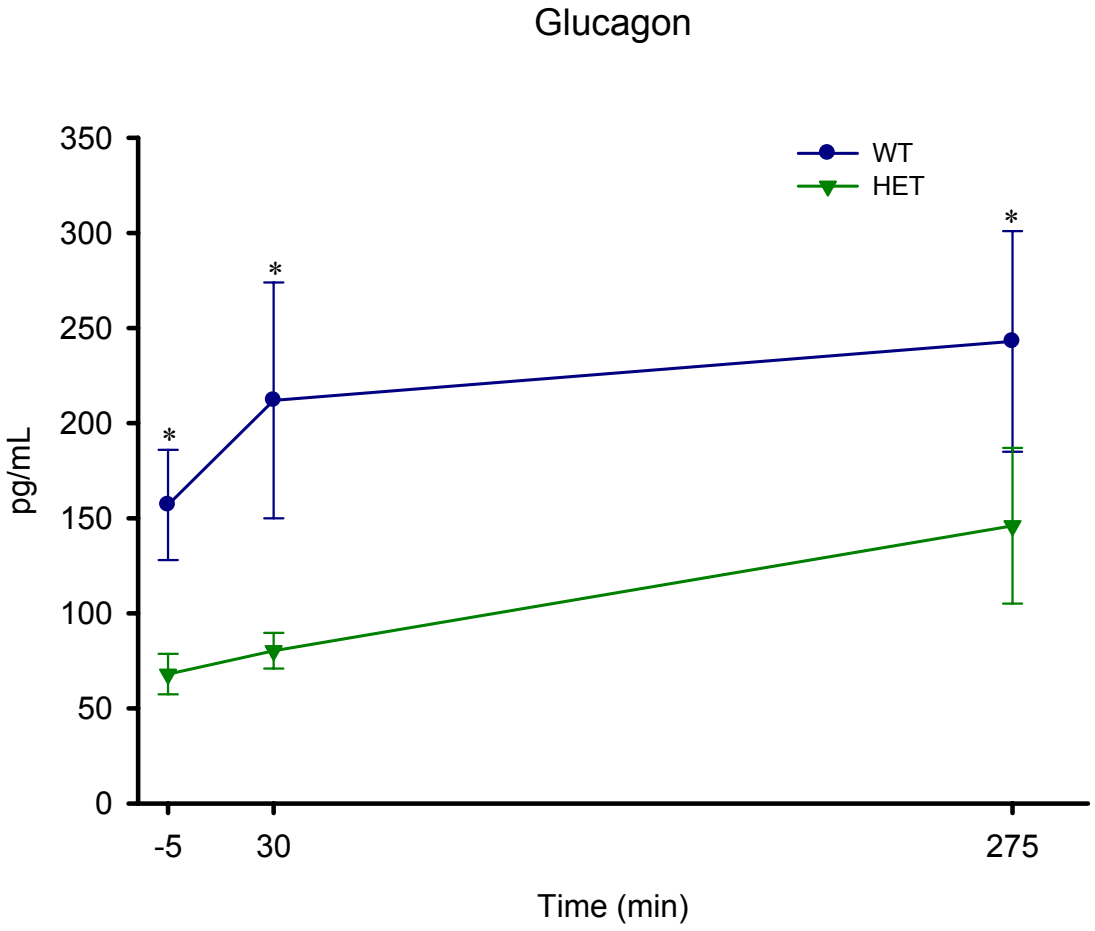

Figure 25: The plasma concentration of glucagon in pg/mL in WT and HET. Data are expressed as mean ± SE. * P<0.050

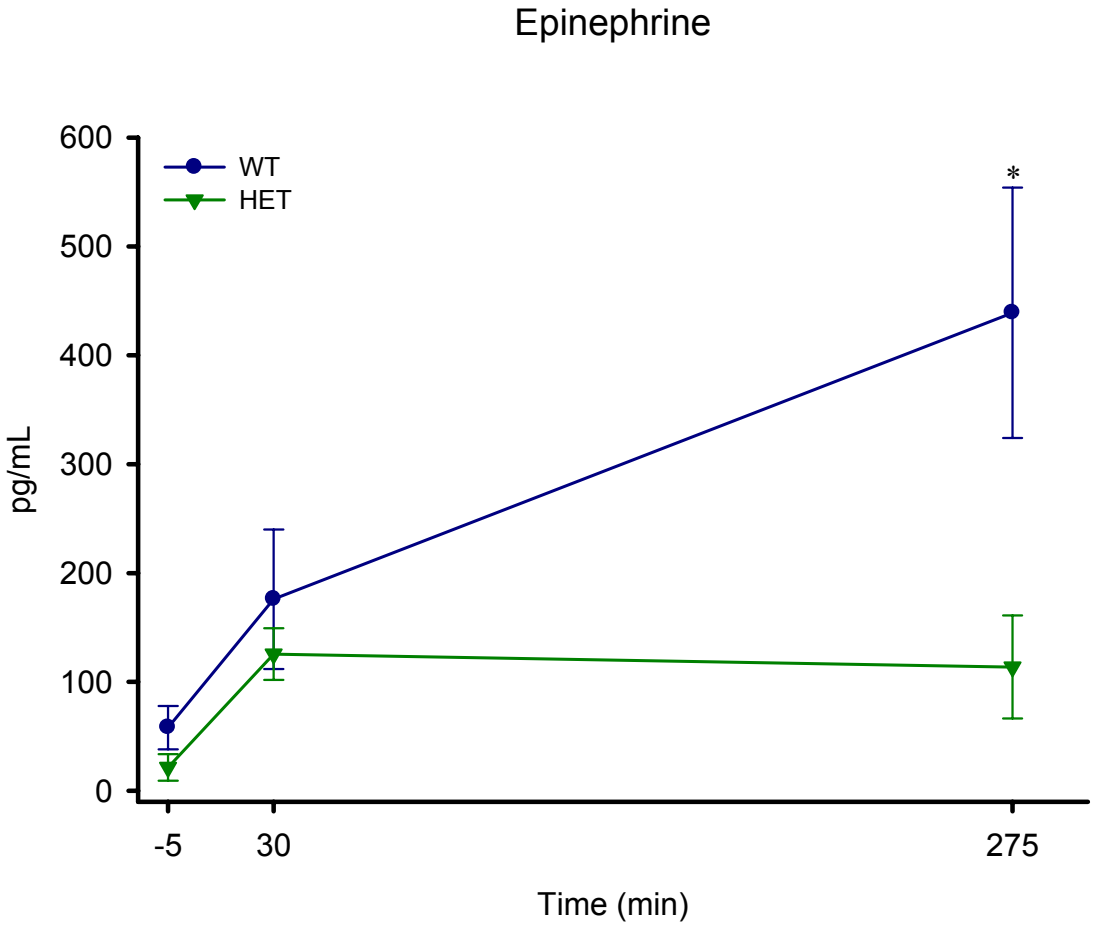

Figure 26: The plasma concentration of epinephrine in pg/mL in WT and HET. Data are expressed as mean ± SE. * P<0.050

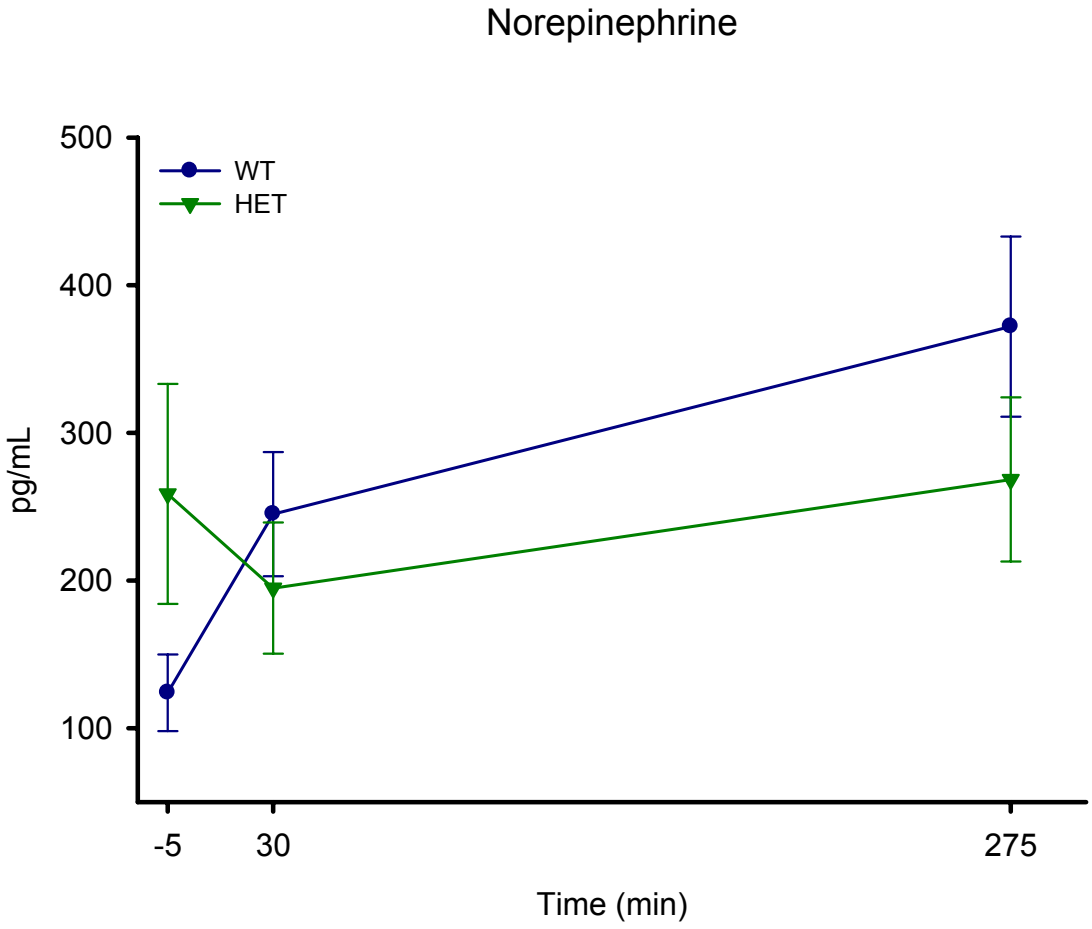

Figure 27: The plasma concentration of norepinephrine in pg/mL in WT and HET. Data are expressed as mean ± SE.

Discussion

It was our hypothesis that the lack of IL-6 would protect against endotoxin-induced hypoglycemia. We based this hypothesis on previously published literature that indicated elevated levels of IL-6 were in part responsible for the exacerbated inflammatory response observed in high dose endotoxemia or sepsis (45,93). Our data indicate that the absence of IL-6 is protective against LPS induced hypoglycemia. We have concluded that the elevation in IL-6 is indirectly responsible for the late stage hypoglycemia associated with endotoxemia.

Most studies assessing metabolic changes in endotoxemia have been conducted in humans and rats. Human studies have shown that endotoxemia results in a hypermetabolic response characterized by an increase in glucose synthesis and release from the liver, leading to a brief state of hyperglycemia coupled with an elevated insulin concentration (20,46). Human studies have also shown that a state of insulin resistance develops in the presence of conditions favorable for gluconeogenesis (22). Our studies revealed that all groups experienced an early transient hyperglycemia, although we did not see an early elevation in insulin. Studies conducted in rats have shown, in addition to an early transient hyperglycemic phase, an end stage severe hypoglycemia occurs primarily because of a subsequent reduction in hepatic R_a (45). This results in part from the eventual impairment in the gluconeogenic capacity and hormonal responsiveness in the liver (45). In our studies, WT mice did not demonstrate a sustained rise in R_a but did exhibit a rise in glucose clearance, the latter being the primary cause of the accompanying hypoglycemia. Other studies in rats have demonstrated an early increase in R_a, glucose recycling, and glucose clearance and this increase was sustained

throughout the four hour study period (78). Due to sample volume constraints, we were not able to obtain enough data during the first 180 min of the study to adequately assess glucose kinetics. Thus, we were not able to determine the time course of the early changes in early R_a, R_d, or glucose clearance in any of our groups. Regardless, the overall response we observed in WT was similar to other species, although the difference in the quantitative response may be dependent on the dose of LPS used.

Although we observed typical pro-inflammatory cytokine responses in WT, we were a bit surprised that TNF-α and IL-1β levels did not wane during the latter portion of the study as previously observed by other groups (2,39,85). A possible explanation for this caveat is that we injected the bolus of LPS into the jugular vein whereas the bolus of LPS is typically introduced intraperitoneally (1,11,15,29,43). This route of administration may have activated these cytokines in a manner that makes it difficult to compare with previously published data. It is also important to note that our animals were surgically prepared 5 – 7 days prior to the study, which may modify the animals' immunological response on our study day. However, it is unlikely that the prior stress can explain the differing response since prior stress diminishes the overall response but does not substantially alter the time course of the response.

Distinguishing between paracrine and endocrine effects associated with IL-6: KO mice have no IL-6 paracrine or endocrine activity whereas WT mice with intact IL-6 production experience an increase in both paracrine and endocrine activity of IL-6 during exposure to LPS. This increase is, in part, mediated through the upregulation of TNF-α observed during the early infection process. As expected, our WT mice had a significant

increase ($P<0.027$) in TNF-α within the first 30 min following the LPS bolus accompanied with a characteristic rise in IL-6 (Fig 10). In contrast, although KO experienced an increase in TNF-α as well, this increase was delayed as compared to WT. As expected, IL-6 levels in KO were not detectable. Since IL-6 can amplify TNF-α transcription, the absence of IL-6 in KO may explain the observed delay in TNF-α response (14). The anti-inflammatory cytokine IL-10 has been associated with the suppression or counterregulatory effects of both IL-6 and TNF-α (29,30,51) and works primarily to help quell the possible detrimental effects of these cytokines (30). Our findings draw a parallel with previous studies in that during early endotoxemia, IL-10 activation has a sluggish response during the time when TNF-α and subsequently IL-6 are first activated in WT (14). There is speculation that the early increase in these pro-inflammatory cytokines may actually suppress the beneficial early activation of IL-10 (30). Interestingly, our KO experienced an early activation of IL-10, and a delayed activation of TNF-α. The absence of IL-6 may have facilitated this early rise. The early activation of IL-10 in KO may be due to the freedom of this cytokine to be upregulated in the absence of the counterregulatory cytokine IL-6. This beneficial effect of IL-10 may be masked or quelled by the overpowering levels of IL-6 frequently observed in endotoxemia. These findings correlate with previous studies conducted where anti-TNF-α antibodies where given prior to a bolus of LPS; IL-6 and IL-1β were blunted whereas IL-10 had an increased early response (12).

rmIL-6 was infused into IL-6 knockout mice in attempt to recreate the endocrine effects of WT IL-6 response to endotoxin. It was our hypothesis that the replacement of IL-6 in KO would restore the IL-1β, TNF-α, and IL-10 response to endotoxin. We found

this not entirely to be the case, although we were successful in recreating the IL-6 profile observed in WT. Infusion of IL-6 did not correct the delayed TNF-α and IL-1β response to endotoxin but it did delay the IL-10 response. A possible explanation may be that activation of TNF-α would not resemble the WT activation until endocrine levels of IL-6 were high enough to trigger the positive feedback response previously mentioned. This can be further validated in the respect that TNF-α levels in the KO + IL-6 group closely mirror the levels observed in WT from 180 min until the end of the study. The paracrine effect of IL-6 is important in regard to TNF-α and IL-1β and could not be recreated by IL-6 infusion alone. KO + IL-6 displayed the same sluggish IL-10 response as seen with WT suggesting that the endocrine effects of IL-6 are an important modulator of the IL-10 response.

As previously mentioned, WT fasting basal glucose were 102±11 ($P<0.005$) whereas KO and KO + IL-6 both had similar fasting basal glucose levels (145±9 and 158±6 mg/dl; respectively). This observation was interesting to us, as recent studies conducted by Di Gregorio *et al.* (26) have concluded that glucose levels in both WT and KO mice after a 4 h fast were similar and both genotypes ranged just below 200 mg/dL. These authors also found that there were no differences in baseline glucose or levels during a glucose tolerance test. This group utilized KO mice on a C57BL/6J background similar to ours, although the Di Gregorio studies utilized animals from Jackson Laboratories whereas this differed from our studies as we used a heterozygote breeding scheme to obtain littermates. The conflicting fasting glucose data observed between our studies and the Di Gregorio studies is interesting in that this may be attributed to intrinsic genetic differences brought about by breeding.

Absence of IL-6 resulted in a more robust early hyperglycemic response to endotoxin and the absence of subsequent hypoglycemia. KO and KO + IL-6 experienced an early transient hyperglycemic phase whereas WT experienced a less intense early transient hyperglycemia. It has been previously observed that endotoxin exposure will induce an early transient hyperglycemic phase and this phase is present in conjunction with elevated insulin levels (20,54,95) and an increase in gluconeogenesis (46). The early increase in glycogenolysis and gluconeogenesis is strongly correlated with an increase in R_a and R_d. Likewise, elevated levels of IL-6 have been associated with high dose endotoxemia and it has been observed that this may contribute to increased R_a and R_d in rats, mice, and humans (16,45,93). With this in mind, we expected to see an increase in R_a and R_d in WT within 60 min, or in conjunction with the increase in IL-6, after giving the bolus of LPS. We did not detect an early increase in R_a following the bolus of endotoxin, but did see the characteristic later increase in clearance. As already mentioned our study was designed to assess glucose kinetics in the later phase of endotoxemia; we could not take enough samples early in the study to adequately assess the rapid shifts in R_a and R_d. Consequently, we were not surprised we did not detect an early rise in R_a. The increase in clearance during the late phase likely explains the fall in glucose in WT by the end of the study. Previous studies conducted in rats have indicated that a decrease in R_a and in gluconeogenesis and concomitant depletion in glycogen stores along with the increase in clearance is likely the cause of the hypoglycemic state observed in late sepsis (16,44). Typically, in late sepsis, insulin is decreased under basal values while epinephrine and glucagon are increased. Our data indicate WT experienced little change in insulin or glucagon by the end of the study while epinephrine increased

substantially ($P<0.001$). One explanation may be that our WT animals were fairly glycogen depleted when basal time point sampling began. Elevated epinephrine levels contribute little to the correction of end stage hypoglycemic glucose values, as previous studies in rats have shown elevated levels of epinephrine were not protective against hypoglycemia (44). An additional possibility is that the dose of endotoxin was modest and did not substantially impair hepatic metabolism.

As previously mentioned, both KO and KO + IL-6 had similar fasting basal glucose concentrations. Both groups experienced an early transient hyperglycemia. We postulated that the infusion of IL-6 into KO animals would recapitulate the immunological and hormonal responses observed in WT. KO + IL-6 displayed a glucose profile similar to KO throughout the entirety of the study, even though there was a delayed response in both TNF-α and IL-10. This is interesting in that it suggests the endocrine actions of IL-6 are not enough to alter glucose metabolism. Another interesting point is that both KO and KO + IL-6 displayed a decrease in clearance in the first 30 min of the study and KO + IL-6 had a profound increase in clearance from 180 min until the end of the study ($P<0.050$). The early decrease in clearance may have contributed to the euglycemia observed at the end of the study by amplifying the hyperglycemia during the early phase. It is important to keep in mind that there was relatively no endocrine IL-6 activity in either group during the timeframe the early decrease in clearance was observed. It is also interesting to note that the substantial increase in clearance in KO + IL-6 from 180 min to 240 min was observed in light of no change in insulin, glucagon, or epinephrine, whereas KO only experienced an increase in glucagon at this timepoint ($P<0.002$).

Quantitative reduction in the IL-6 gene alters metabolic and immunologic properties: To our knowledge, there have been no previous studies in which heterozygous IL-6 knockout mice have been utilized to assess metabolic or immunologic parameters. We have found that HET mice have an intermediate metabolic and immunologic response to a challenge of endotoxin. Even though HET mice have one copy of the IL-6 gene, it was clear that endocrine levels of IL-6 remained undetectable 30 min after injection of LPS. This is interesting in that WT mice experienced a typical rapid increase in IL-6 by this time. By the 180 min sample, HET IL-6 levels were comparable to those seen in WT and remained elevated for the remainder of the study. One theory is that the IL-6 protein concentration must increase to a maximal level within the local interstitial compartment where it is produced before it is able spill into the extracellular space and subsequently into the circulation. Thus, paracrine mediated effects of TNF-α and IL-6 must be at its maximum threshold in order to facilitate adequate endocrine activity. This would be a logical order of events in that WT mice have a rapid rise in IL-6 due to the presence of two copies of the IL-6 allele whereas HET mice only have one allele and would be more dependent on time to increase the transcription cascade to produce substantial enough levels of IL-6 in the interstitial space. Interestingly, the TNF-α profile in HET closely mirrors the pattern seen in the KO in that there was a 50% blunted response to LPS compared to WT. Again, this could be due to the early absence of increased IL-6 endocrine activity. IL-10 also had a sluggish response to LPS in HET. When examining the cytokine profile of HET mice, it is clear that the immunological response does not resemble the patterns observed with WT, but rather most closely resembles KO + IL-6. Our findings indicate that the quantitative reduction in the IL-6 gene causes a more

sluggish pro-inflammatory cytokine response and does not alter the anti-inflammatory response as compared to WT.

HET exhibited a dramatic early transient hyperglycemic phase and began to experience a reduction in arterial glucose (82.2±3.7 mg/dl) by the last sample of the study. This could suggest, since KO appear to be protected against hypoglycemia, partial loss of IL-6 protein in HET may be of some benefit in protecting against hypoglycemia as well. R_a and R_d in HET did not change throughout the study, similar to patterns observed in WT, although fasting glucose was substantially higher in HET than WT ($P<0.005$). However, glucose clearance in HET had a much different pattern than WT, in that clearance increased significantly from 180 min until the end of the study ($P<0.008$). This increase in clearance was similar to the pattern observed in KO. This is interesting in that HET mice experienced modest changes in insulin, glucagon, or epinephrine throughout the study and did not become hypoglycemic, whereas WT were in fact hypoglycemic and had elevated epinephrine levels at the end of the study. Given that HET appeared to most closely resemble the intermediate responses observed with KO + IL-6, it is likely that the early and complete endocrine IL-6 response to endotoxin is necessary to facilitate the inflammatory state typically associated with sepsis.

The genetic manipulation of our animals may have inadvertently interfered with glucose absorption kinetics, thus altering the fasting glucose profile of our animals. Other studies suggest that IL-6 can exert metabolic effects (29,34,40,74,84). Our data indicate that KO animals were likely insulin resistant after a 5 h fast. This finding is in contrast to studies performed by *Kim et al.* (37); IL-6 infusion had no effect on basal metabolism and caused hepatic insulin resistance. It can be speculated that the Kim

group did not observe changes in metabolism as a result of the IL-6 infusion, but rather metabolism was only affected when mice were challenged with insulin (37). Moreover, our infusion of IL-6 did not alter the insulin, glucagon, epinephrine, or norepinephrine response to endotoxin. This can be attributed to the fact that IL-6 levels used in our studies were physiologically correlated with levels observed in WT mice during endotoxemia. A conclusion that can be drawn from this contrast in data is that in the setting of endotoxemia, the role of IL-6 is different from when challenged with insulin.

In conclusion, KO appeared to be protected against endotoxin-induced hypoglycemia. This observation is made in conjunction with elevated baseline glucose in all mice lacking either one or both copies of the IL-6 gene. It is possible the early alterations between glycemic variables and cytokines allowed for the late term protective effects against hypoglycemia. This was in conjunction with the stabilization in arterial glucose at the end of the study. Our data suggest end stage glucose levels observed in KO may be attributed to factors other than hormonal catabolic mediators such as glucagon, epinephrine, and norepinephrine. This observation, coupled with the previously stated glucose kinetics profile, leads us to believe that carbohydrate metabolism is not altered directly through the properties of the IL-6 protein, although our studies indicate IL-6 is partly but not entirely responsible for the metabolic and immunologic profile seen during high dose endotoxemia. Likewise, the WT metabolic and immunologic response could not be recreated in the IL-6 replacement group. This leads us to believe that metabolic and immunologic changes observed during endotoxemia occur indirectly through either an IL-6 mediated transcription pathway or through a redundant immunological signaling pathway that includes IL-6.

REFERENCES

1. Aderka D, Le J, Vilcek J. IL-6 inhibits lipopolysaccharide-induced tumor necrosis factor production in cultured human monocytes, U937 cells and in mice. *J Immunol* 143: 3517-3523 , 1989

2. Andus A, Bauer J, Gerok W. Effects of cytokines on the liver. *Hepatology* 13: 364-375, 1991

3. Angus DC, Linde-Zwirble WT, Lidicker J, Clermont G, Carcillo J, Pinsky MR. Epidemiology of severe sepsis in the Untied States: analysis of incidence, outcome, and associated cost of care. *Crit Care Med* 29: 1303-1310, 2001

4. Anton AH and Sayre DF. A study of the factors affecting the aluminum oxidetrihydroxyinle procedure for the analysis of catecholamines. *J Pharm Exp Ther* 138: 360-375, 1962

5. Apantaku FO, Foe LG, Schumer W. Hepatic fructose-2,6-bisphosphate in rats with peritonitis and septic shock. *Surgery* 96: 770-773, 1984

6. Ardawi MSM, Ashy AA, Jamal YS, Khoja JM. Metabolic control of hepatic gluconeogenesis in response to sepsis. *J Lab Clin Med* 114: 566-579, 1992

7. Bagby GJ, Lang CH, Hargrove DM, Thompson JJ, Wilson LA, Spitzer JJ. Glucose kinetics in rats infused with endotoxin-induced monokines or tumor necrosis factor. *Circ Shock* 24: 111-121, 1988

8. Bankey PE, Mazuski JE, Ortiz M, Fulco JM, Cerra FB. Hepatic acute phase protein synthesis is indirectly regulated by tumor necrosis factor. *J Trauma* 30: 1181-1188, 1990

9. Bautista AP, Spolarics Z, Jaeschke H, Smith CW, Spitzer JJ. Monoclonal antibody against the CD18 adhesion molecule stimulates glucose uptake in the liver by hepatic nonparenchymal cells. *Hepatology* 17: 924-031, 1993

10. Bernard GR, Vincent JL, Laterre PF, LaRosa SP, Dhainaut JF, Lopez-Rodriguez A, Steingrub JS, Garber GE, Helterbrand JD, Ely EW. Efficacy and safety of recombinant human activated protein C for severe sepsis. *N Engl J Med* 344: 699-709, 2001

11. Berry LJ, Smythe DS, Young LG. Effects of bacterial endotoxin on metabolism I. Carbohydrate depletion and the protective role of cortisone. *J Exp Med* 110: 389-405, 1959

12. Beutler B, Milsark IW, Cerami A. Passive immunization against cachectin/tumor necrosis factor protects mice from lethal effects of endotoxin. *Science* 229: 869-871, 1985

13. Bone RC, Balk RA, Cerra FB. Definition of sepsis and organ failure and guidelines for the use of innovative therapies in sepsis. *Chest* 101: 1644-1655, 1992

14. Bone RC, Grodzin CJ, Balk RA. Sepsis: A new hypothesis for pathogenesis of the disease process. *Chest* 112: 235-243 , 1997

15. Braude AI, Carey FJ, Sutherland D, Zalesky M. Studies with radioactive endotoxin. I. The use of Cr^{51} to label endotoxin of *E. coli. J Clin Invest* 34: 850, 1955

16. Buday AZ, Lang CH, Bagby GJ, Spitzer JJ. Glycogen synthase and phosphorylase activities during glycogen repletion in endotoxemic rats. *Circ Shock* 19: 149-163, 1986

17. Casteleijn E, Kuipers J, Van Rooij HC,Kamps JA, Koster JF, van Berkel TJ. Endotoxin stimulates glycogenolysis in the liver by means of intercellular communication. *J Biol Chem* 263: 6953-6955, 1988

18. Cerra FB. Hypermetabolism, organ failure, and metabolic support. *Surgery* 101 (1): 1-14

19. Cerra FB, Siegel JH, Border JR, Wiles J, McMenamy RR. The hepatic failure of sepsis: cellular vs. substrate. *Surgery* 86: 409-422, 1979

20. Clemens MG, Chaudry IH, Daigneau N, Baue AE. Insulin resistance and depressed gluconeogenic capability during early hyperglycemic sepsis. *J Trauma* 24 (8): 701-708, 1984

21. Clemens MG, Chaundry IH, McDermott PH, Baue AE. Regulation of glucose production from lactate in experimental sepsis. *Am J Physiol* 244: R794-R800, 1983

22. Curnow RT, Rayfield EJ, George DT, Zenser TV, DeRubertis FR. Altered hepatic glycogen metabolism and glucoregulatory hormones during sepsis. *Am J Physiol* 230: 1296-1301, 1976

23. de Bodo RC, Steele R, Altszuler N, Dunn A, Bishop JS. On the hormonal regulation of carbohydrate metabolism: Studies with ^{14}C glucose. *Recent Prog Horm Res* 19: 445-488, 1963

24. Decker K. Biologically active products of stimulated liver macrophages (Kupffer cells). *Eur J Biochem* 192: 245-261, 1990

25. Deutschman CS, DeMaio A, Clemens MG. Sepsis-induced attenuation of glucagon and 8-BrcAMP modulation of the phosphoenolpyruvate carboxykinase gene. *Am J Physiol* 269: R584-R591, 1995

26. Di Gregorio GB, Hensley L, Lu T, Ranganathan G, Kern PA. Lipid and carbohydrate metabolism in mice with a targeted mutation in the IL-6 gene: absence of development of age-related obesity. *Am J Physiol* 287: E182-187, 2004

27. Doi F, Goya T, Torisu M. Potential role of hepatic machrophages in neutrophil-mediated liver injury in rats with sepsis. *Hepatology* 17: 1086-1094, 1993

28. Ferguson JL, Spitzer JJ, Miller HI. Effects of endotoxin on regional blood flow in the unanesthetized guinea pig. *J Surg Res* 25: 236-243, 1978

29. Frost RA, Nystrom GJ, Lang CH. Lipopolysaccharide and proinflammatory cytokines stimulate interleukin-6 expression in C2C12 myoblasts: role of the Jun NH2-terminal kinase. *Am J Physiol* 285: R1153-R1164, 2003

30. Gerard C, Bruyns C, Marchant A, Abramowicz D, Vandenabeele P, Delvaux A, Fiers W, Goldman M, Velu T. Interleukin-10 reduces the release of tumor necrosis factor and prevents lethality in experimental endotoxemia. *J Exp Med* 177: 547-550 , 1993

31. Goldstein DS, Feuerstein G, Izzo,Jr JL, Kopin IJ, Keiser HR. Validity and reliability of liquid chromatography with electrochemical detection for measuring plasma levels of norepinephrine and epinephrine in man. *Life Sci* 28: 467-475, 1981

32. Grisham MB, Everse J, Janssen HF. Endotoxemia and neutrophil activation in vivo. *Am J Physiol* 254 (23): H1017-H1022, 1988

33. Hamosh M, Shapiro B. The mechanism of glycogenolytic action of endotoxin. *Br J Exp Pathol* 4: 372-380, 1960

34. Heinrich PC, Castell JV, Andus T. Interleukin-6 and the acute phase response. *Biochem J* 265: 621-636, 1990

35. Hesse DG, Tracey KJ, Fong Y, Manogue KR, Palladino MA, Cerami A, Shires GT, Lowry SF. Cytokine appearance in human endotoxemia and primate bacteremia. *Surgery Gyn Obs* 166: 147-153 , 1988

36. Imamura M, Clowes GHA, Blackburn GL, O'Donnell TF, Trerice M, Bhimjee Y, Ryan NT. Liver metabolism and gluconeogenesis in trauma and sepsis. *Surgery* 77: 868-880, 1975

37. Kim HJ, Higashimori T, Park SY, Choi H, Dong J, Kim YJ, Noh HL, Cho YR, Cline G, Kim YB, Kim JK. Differential effects of interleukin-6 and -10 on skeletal muscle and liver insulin action in vivo. *Diabetes* 53: 1060-1067, 2004

38. Klapproth J, Castell J, Geiger T, Andus T, Heinrich PC. Fate and biological action of human recombinant interleukin-1β in the rat in vivo. *Eur J Immunol* 19: 1485-1490, 1989
39. Kishimoto T, Akira S, Narazaki M, Taga T. Interleukin-6 family of cytokines and gp130. *Blood* 86: 1243-1254 ,1995

40. Klover PJ, Zimmers TA, Koniaris LG, Mooney RA. Chronic exposure to interleukin-6 causes hepatic insulin resistance in mice. *Diabetes* 52: 2784-2789, 2003

41. Kopf M, Baumann H, Freer G, Freudenberg M, Lamers M, Kishimoto T, Zinkernagel R, Bleuthmann H, Kohler G. Impaired immune and acute-phase responses in interleukin-6-deficient mice. *Nature* 368: 339-342, 1994

42. Kraegen EW, James DE, Jenkins AB, Chrisholm DJ. Does-response curves for in vivo insulin sensitivity in individual tissues in rats. *Am J Physiol* 248: E353-E362, 1985

43. Lang CH, Bagby GJ, Dobrescu C, Ottlakan A, Spitzer JJ. Sepsis- and endotoxin-induced increase in organ glucose uptake in leukocyte-depleted rats. *Am J Physiol* 263: R1324-R1332, 1992

44. Lang CH, Dobrescu C, Hargrove DM, Bagby GJ, Spitzer JJ. Attenuation of endotoxin-induced increase in glucose metabolism by platelet-activating factor antagonist. *Circ Shock* 23: 179-188, 1987

45. Lang CH, Spolarics Z, Ottlakan A, Spitzer JJ. Effect of high-dose endotoxin on glucose production and utilization. *Metabolism* 42 (10): 1351-1358, 1993

46. Long CL, Kinney JM, Geiger JW. Non-suppressability of gluconeogenesis by glucose in septic patients. *Metab Clin Exp* 25: 193-201, 1976

47. Maitra SR, Gestring ML, El-Maghrabi MR, Lang CH, Henry MC. Endotoxin-induced alterations in hepatic glucose-6-phosphatase activity and gene expression. *Mol Cell Biochem* 196: 79-83, 1999

48. Maitra SR, Pan W, Lange AJ, El-Maghrabi MR, Abumrad NN, Pilkis SJ. Glucose-6-phosphatase gene expression and activity are modulated in hemorrhagic shock: Evidence for a new heat sensitive activator. *Biochem Biophys Res Commun* 204: 716-724, 1994

49. Marchant A, Bruyns C, Vandenabeele P, Ducarme M, Gerard C, Delvaux A, DeGroote P, Abramowicz D, Velu T, Goldman M. Interleukin-10 controls interferon-gamma and tumor necrosis factor production during experimental endotoxemia. *Eur J Immunol* 24: 1167-1171 , 1994

50. Mari A, Butler PC, Caumo A, Rizza RA, Cobelli C, Bergman RN, Steil GM. On the calculation of glucose rate of disappearance in nonsteady state. *Am J Physiol* 29: E825-E828, 1994

51. Marsik C, Mayr F, Cardona F, Dehaschnig U, Wagner OF, Jilma B. Endotoxemia modulates toll-like receptors on leukocytes in humans. *Br J Haematol* 121 (4): 653-656, 2003

52. Mathison JC, Ulevitch RJ. The clearance, tissue distribution, and cellular localization of intravenously injected lipopolysaccharide in rabbits. *J Immunol* 123: 2133-2143, 1979

53. McCallum RE, Berry LJ. Mouse liver fructose-1,6-diphosphatase and glucose-6-phosphatase activities after endotoxin poisoning. *Infect Immunity* 6 (5): 883-885, 1972

54. Menten ML, Manning HM. Blood sugar studies on rabbits infected with organisms of the enteritidis-paratyphoid B Group. *J Med Research* 44: 675, 1924

55. Meszaros K, Bagby GJ, Lang CH, Spitzer JJ. Increased uptake and phosphorylation of 2-deoxyglucose by skeletal muscles in endotoxin-treated rats. *Am J Physiol* 253: E33-E39, 1987

56. Meszaros K, Bojta J, Bautista AP, Lang CH, Spitzer JJ. Glucose utilization by Kupffer cells, endothelial cells, and granulocytes in endotoxemic rat liver. *Am J Physiol* 260: G7-G12, 1991

57. Meszaros K, Lang CH, Bagby GJ, Spitzer JJ. Contribution of different organs to increased glucose consumption after endotoxin administration. *J Biol Chem* 262 (23): 10965-10970, 1987

58. Meszaros K, Lang CH, Bojta J, Spitzer JJ. Early changes in glucose utilization of individual tissues after endotoxin administration. *Circ Shock* 29: 108-114, 1989

59. Morgan HE, Cadenas E, Regen DM, Park CR. Regulation of glucose uptake in muscle II. Rate-limiting steps and effects of insulin and anaoxia in hear muscle of diabetic rats. *J Biol Chem* 236: 262-268, 1961

60. Myers SR, Biggers DW, Neal DW, Cherrington AD. Intraportal glucose delivery enhances the effects of hepatic glucose load on net hepatic glucose uptake in vivo. *J Clin Invest* 88: 158-167, 1991

61. Mortensen RF, Shapiro J, Lin B-F, Douches S, Neta R. Interaction of recombinant IL-1 and recombinant tumor necrosis factoring the induction of mouse acute phase proteins. *J Immunol* 140: 2260-2266, 1988

62. Natanson C, Danner RL, Reilly JM. Antibiotics versus cardiovascular support in a canine model of human septic shock. *Am J Physiol* 150: H1440-H1447, 1990

63. Okusawa S, Gelfland JA, Ikejima T, Connolly RJ, Dinarello CA. Interleukin-1 induces a shock-like state in rabbits. Synergism with tumor necrosis factor and the effect of cyclooygenase inhibition. *J Clin Invest* 81: 1162-1172 , 1988

64. Opal SM. Clinical trial design and outcomes in patients with severe sepsis. *Shock* 20 (4): 295-302, 2003

65. Pajkrt D, Camoglio L, Tiel-van Buul MC, de Bruin K, Cutler DL, Affrime MB, Rikken G, van der Poll T, ten Cate JW, van Deventer SJ. Attenuation of the proinflammatory response by recombinant human IL-10 in human endotoxemia; the effect of timing of rhIL-10 administration. *J Immunol* 158: 3971-3977 , 1997

66. Pajkrt D, van der Poll T, Levi M, Cutler DL, Affrime MB, van den Ende A, ten Cate JW, van Deventer SJ. Interleukin-10 inhibits activation of coagulation and fibrinolysis during human endotoxemia. *Blood* 89: 2701-2705 , 1997

67. Pastor CM, Billiar TR, Losser M-R, Payen DM. Liver injury during sepsis. *J Crit Care* 10 (4): 183-197, 1995

68. Pugin J, Schurer-Maly C-C, Leturcq D, Moriarty A, Ulevitch RJ, Tobias PS. Lipopolysaccharide activation of human endothelial and epithelial cells is mediated by lipopolysaccharide-binding protein and soluble CD-14. *Proc Natl Acad Sci USA* 90: 2744-2748, 1993

69. Raymond RM, Harkema JM, Emerson TE. Mechanism of increased glucose uptake by skeletal muscle during E. coli endotoxin shock in the dog. *Circ Shock* 8: 77-93, 1981

70. Riedemann NC, Neff TA, Guo R-F, Bernacki KD, Laudes IJ, Sarma JV, Lambris JD, Ward PA. Productive effects of IL-6 blockade in sepsis are linked to reduced C5a receptor expression. *J Immunol* 170: 503-507, 2003

71. Romanosky AJ, Bagby GJ, Bockman EL, Spitzer JJ. Increased muscle glucose uptake and lactate release after endotoxin administration. *Am J Physiol* 239: E311-E316, 1980

72. Roth BL, Spitzer JA. Shift from alpha- to beta-type adrenergic receptor-mediated responses in chronically endotoxemic rats. *Am J Physol Endocrinol Metab* 252 (15): E699-E702, 1987

73. Schlayer HJ, Kark U, Ganter U, Hermann R, Decker K. Enhancement of neutrophil adherence to isolated rat liver sinusoidal endothelial cells by supernatants of

lipopolysaccharide-activated monocytes: Role of tumor necrosis factor. *J Hepatol* 5: 311-321, 1987

74. Senn JJ, Klover PJ, Nowak IA, Mooney RA. Interleukin-6 induces cellular insulin resistance in hepatocytes. *Diabetes* 51: 3391-3399, 2002

75. Sharma RJ, Macallan DC, Sedwick P, Remick DG, Griffin GE. Kinetics of endotoxin-induced acute-phase protein gene expression and its modulation by TNF-α monoclonal antibody. *Am J Physiol* 262: R786-R793, 1992

76. Somogyi, M. Determination of blood sugar. *J Biol Chem* 160: 69-73, 1945

77. Sonne O, Davidsen O, Moller BK, Munck Peterson C. Cellular targets and receptors for interleukin-6. I. In vivo and in vitro uptake of IL-6 in liver and hepatocytes. *Eur J Clin Invest* 20: 366-370, 1990

78. Spitzer JJ, Bagby GJ, Meszaros K, Lang CH. Altered control of carbohydrate metabolism in endotoxemia. *Mol Cell Mech Sep Shock* 145-165, 1989

79. Stith RD, Luo J. Endocrine and carbohydrate responses to interleukin-6 in vivo.

80. Su GL, Freeswick PD, Geller DA, Wang Q, Shapiro RA, Wan YH, Billar TR, Tweardy DJ, Simmons RL, Wang SC. Molecular cloning, characterization, and tissue distribution of rat lipopolysaccharide binding protein: Evidence for extrahepatic expression. *J Immunol* 153: 743-752, 1994

81. Tilg H, Trehu E, Atkins MB, Dinarello CA, Mier JW. Interleukin-6 (IL-6) as an anti-inflammatory cytokine: Induction of circulating IL-1 receptor antagonist and soluble tumor necrosis factor receptor p55. *Blood* 83: 113-118, 1994

82. Tobias PS, Soldau K, Ulevitch RJ. Isolation of a lipopolysaccharide-binding acute phase reactant from rabbit serum. *J Exp Med* 164: 777-793, 1986

83. Tracey KJ, Beutler B, Lowry SF, Merryweather J, Wolpe S, Milsark IW, Hariri RJ, Fahey TJ, Zentella A, Albert JD *et al.*. Shock and tissue injury induced by recombinant human cachectin. *Science* 234: 470-474 , 1986

84. Tsigos C, Papanicolaou DA, Kyrou I, Defesnsor R, Mitsiadis CS, Chrousos GP. Dose-dependent effects of recombinant human interleukin-6 on glucose regulation. *J Clin Endocrinol Metab* 82: 4167-4170, 1997

85. Ulich TR, Guo K, Yin S, del Castillo J, Yi ES, Thompson RC, Eisenberg SP. Endotoxin-induced cytokine gene expression in vivo. IV. Expression of interleukin-1α/β and interleukin-1 receptor antagonist mRNA during endotoxemia and during endotoxin-initiated local acute inflammation. *Am J Pathol* 141: 61-68, 1992

86. van den Berghe G, Wouters PJ, Bouillon R, Weekers F, Verwaest C, Schetz M, Vlasselaers D, Ferdinande P, Lauwers P. Outcome benefit of intensive insulin therapy in the critically ill: insulin dose versus glycemic control. *Crit Care Med* 31: 359-366, 2003

87. van den Berghe G, Wouters PJ, Weekers F, Verwaest C, Bruyninckx F, Schetz M, Vlasselaers D, Ferdinande P, Lauwers P, Bouillon R. Intensive insulin therapy in critically ill patients. *N Engl J Med* 345: 1359-1367, 2001

88. van der Poll T, Buller HR, ten Cate H, Wortel CH, Bauer KA, van Deventer SJ, Hack CE, Sauerwein HP, Rosenberg RD, ten Cate JW. Activation of coagulation after administration of tumor necrosis factor to normal subjects. *N Engl J Med* 322: 1622-1627 , 1990

89. van der Poll T, Lowry SF. Endogenous mechanisms regulating TNF and IL-1 during sepsis. In Vincent JL (ed): Yearbook of Intensive Care and Emergency Medicine. New York, Springer-Verlag, 1995, p 385

90. van der Poll T, van Deventer SJH, Hack CE, Wolbink GJ, Aarden LA, Buller HR, ten Cate JW. Effects on leukocytes following injection of tumor necrosis factor into healthy humans. *Blood* 79: 693-698 , 1992

91. Vogel SN, Henricson BE, Neta R. Roles of interleukin-1 and tumor necrosis factor in lipopolysaccharide-induced hypoglycemia. *Infect Immun* 59: 244-2498, 1991

92. Wall JS, Steele R, de Bodo RC, Altszuler N. Effect of insulin on utilization and production of circulating glucose. *Am J Physiol* 189: 43-50, 1957

93. Wheeler AP, Bernard GR. Treating patients with severe sepsis. *N Engl J Med* 340 (3): 207-214, 1999

94. Whitthaut R, Farhood A, Smith CW, Jaeschkett H. Complement and tumor necrosis factor-α contribute to MAC-1 (CDllb/CD18) up-regulation and systemic neutrophil activation during endotoxemia in vivo. *J Leukoc Biol* 55: 105-111, 1994

95. Zeckwer IT, Goodell H. Blood sugar changes in fatal bacterial anaphylaxis in the rabbit. *J Exp Med* 42: 43, 1925

96. Zeni F, Freeman B, Natanson C. Anti-inflammatory therapies to treat sepsis and septic shock: a reassessment. *Crit Care Med* 25: 1095-1100, 1997

97. Zhang P, Xie M, Spitzer JA. Hepatic neutrophil sequestration in early sepsis: Enhanced expression of adhesion molecules and phagocytic activity. *Shock* 2: 133-140, 1994